A FLUORESCENCE STUDY OF HORSE PLASMA GELSOLIN LABELLED WITH 6-ACRYLOYL-2-DIMETHYLAMINONAPTHALENE

By

SCOTT WILLIAM REID

B.Sc. Robert Gordon's Institute of Technology, 1988

A THESIS SUBMITTED IN PARTIAL FULFILLMENT

OF THE REQUIREMENTS FOR THE DEGREE OF

MASTER OF SCIENCE

IN

THE FACULTY OF GRADUATE STUDIES

(Department of Chemistry)

We accept this thesis as conforming

to the required standard

THE UNIVERSITY OF BRITISH COLUMBIA

NOVEMBER 1990

In presenting this thesis in partial fulfilment of the requirements for an advanced degree at the University of British Columbia, I agree that the Library shall make it freely available for reference and study. I further agree that permission for extensive copying of this thesis for scholarly purposes may be granted by the head of my department or by his or her representatives. It is understood that copying or publication of this thesis for financial gain shall not be allowed without my written permission.

Department of Chemistry

The University of British Columbia
Vancouver, Canada

Date 6/12/90

DE-6 (2/88)

Abstract

Gelsolin was labelled with the sulphydryl-specific fluorescent reagent 6-acryloyl-2-dimethylaminonaphthalene (acrylodan). The degree of labelling using non-denaturing conditions was 1.9 ± 0.5 acrylodans per gelsolin molecule. Circular dichroism and viscosity studies showed no significant effect on gelsolin structure and function on incorporation of the label.

Circular dichroism studies did not detect Ca^{2+} effects on acrylodan-labelled gelsolin, but fluorescence studies detected subtle changes in the protein. The presence of Ca^{2+} causes a decrease and red-shift in fluorescence emission, an increase in sensitivity to quenching by I^- and a decrease in fluorescence polarisation of the acrylodan-labelled gelsolin. These indicate an increased degree of exposure of the fluorescent label to the solvent environment on interaction of gelsolin with Ca^{2+}.

Actin binding to gelsolin was evident from a decrease in fluorescence intensity, an increase in sensitivity to quenching and an increase in fluorescence polarisation. Actin binding increases the exposure of the acrylodan label to solvent, as does Ca^{2+} binding.

Table of Contents

List of Tables

List of Figures

Acknowledgement

I would like to thank Dr Leslie D Burtnick for his guidance and encouragement throughout this project. I would also like to thank Robert Robinson and Ian Clark for the interest they have shown in this project and for their part in the collection of horse plasma.

Abbreviations

Acrylodan	6-acryloyl-2-(dimethylamino)naphthalene
ACRG	Acrylodan labelled Gelsolin
ATP	Adenosine 5'-Triphosphate
CD	Circular Dichroism
DEAE-Sephadex	Diethylaminoethyl-Sephadex
DBP	Vitamin D-Binding Protein
DMF	*N*,*N*-Dimethylformamide
DMSO	Dimethylsulphoxide
DTT	Dithiothreitol
EDTA	Ethylenediaminetetra-acetic acid (disodium salt)
EGTA	Ethylenebis(oxyethylenenitrilo)-tetraacetic acid
Gu-HCl	Guanidine Hydrochloride
PIP_2	Phosphatudylinositol 4,5-bis-phosphate
PMSF	Phenylmethylsulphonyl Fluoride
SDS	Sodium Dodecyl Sulphate
TEMED	*N*,*N*,*N*',*N*'-Tetramethylethylenediamine
Tris	Tris(hydroxymethyl)methylamine
TM	Tropomyosin
TN	Troponin
Buffer A	2mM Tris-HCl, 0.2mM $CaCl_2$, 0.2mM ATP, 1.0mM DTT, pH 8.0.
Buffer I	25mM Tris-HCl, 1mM EGTA, 1mM NaN_3, pH 8.0.

1. INTRODUCTION

PART 1: PROTEINS

1.1.1 Introduction to Actin

Actin is one of the most abundant proteins in nature, making up about 25% of all protein in muscle cells and, typically, 10 - 20% of all protein in eukaryotic non-muscle cells. It was first isolated from muscle tissue by Straub (1942).

This protein undergoes polymerisation from the monomeric G-actin to a long, helical, double-stranded polymer, F-actin (figure 1), under the influence of physiological ionic strength (0.1M KCl) or by the addition of divalent cations (2mM Mg^{2+}) (Tellam and Frieden, 1982). Each actin monomer is a 42 kDa globular protein and filamentous F-actin has a diameter of 70 Å. The structure repeats itself at intervals of 360 Å along the helix axis.

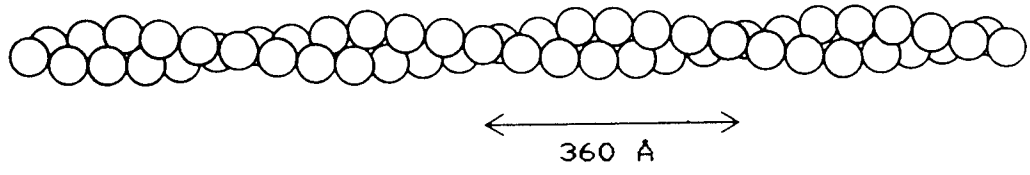

Figure 1: Schematic diagram of the helical array of actin monomers in F-actin (Stryer, 1981).

An arrowhead pattern appears in electron micrographs (figure 2) of F-actin filaments decorated with proteolytic fragments of the contractile protein myosin, indicating the polarity of the filament.

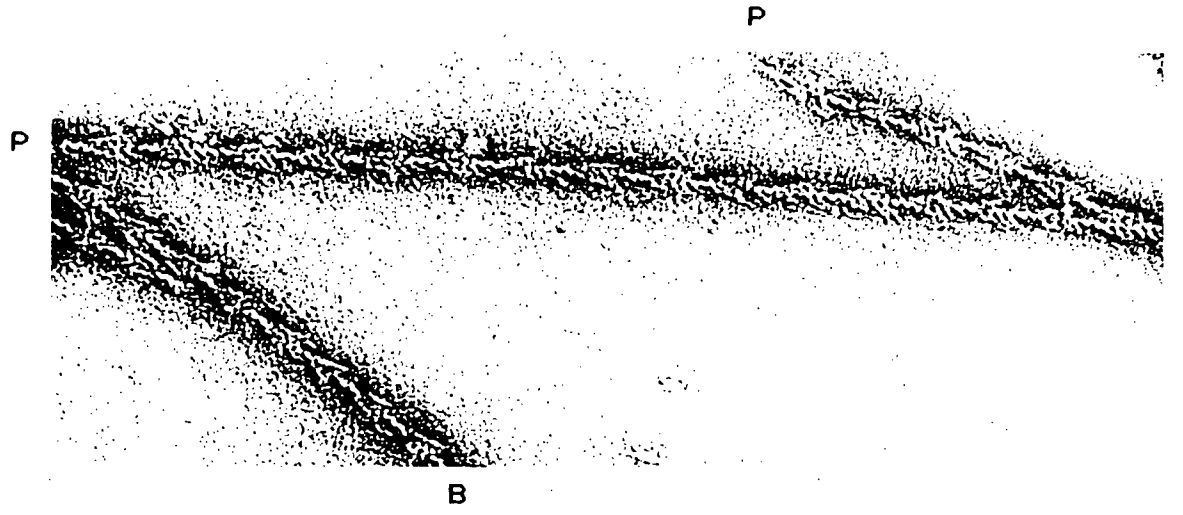

Figure 2: Electron micrograph of filaments of F-actin decorated with proteolytic fragments of the contractile protein myosin. The 'pointed' and 'barbed' ends are represented by P and B, respectively (Stryer, 1981).

1.1.2 Polymerisation of Actin

The polymerisation of actin physiologically is accompanied by, but does not require, hydrolysis of one molecule of bound ATP to one molecule of bound ADP for every monomeric actin subunit. There are two distinct steps involved in polymerization. Firstly, nucleation of polymer growth requires formation of a trimer (Kasai et al., 1960). Nucleation is slow and is the rate limiting step. Secondly, elongation occurs when monomers bind to the ends of the

nuclei to form filaments. The affinity and exchange rate of actin monomers with the 'barbed' end are an order of magnitude higher than at the 'pointed' end.

1.1.3 Location of Actin

Every cell in our bodies possesses actin filaments built into a variety of subcellular machinery. The muscles with which we move, the delicate stereocilia we need to hear and the microvilli that absorb nutrients from our last meal all share the common element of the actin filament (De Rosier, 1990).

Vertebrate striated muscle is composed of thin and thick filaments which slide past one another in the process of muscle contraction. The thin filament (figure 3) is formed by actin, tropomyosin (TM) and one each of the three troponin components, (TN), with actin making up the backbone of the structure. Along each of the two grooves in the F-actin helix lies a TM filament, formed by head-to-tail polymerization of TM. Each TM spans seven actin monomers and the TM filament extends the length of the thin filament. Troponin binds periodically along the TM filament and is a complex of three polypeptides, TN-C (calcium binding), TN-I (inhibitory) and TN-T (TM binding). The TM + TN proteins form the calcium sensitive regulatory switch in striated muscle.

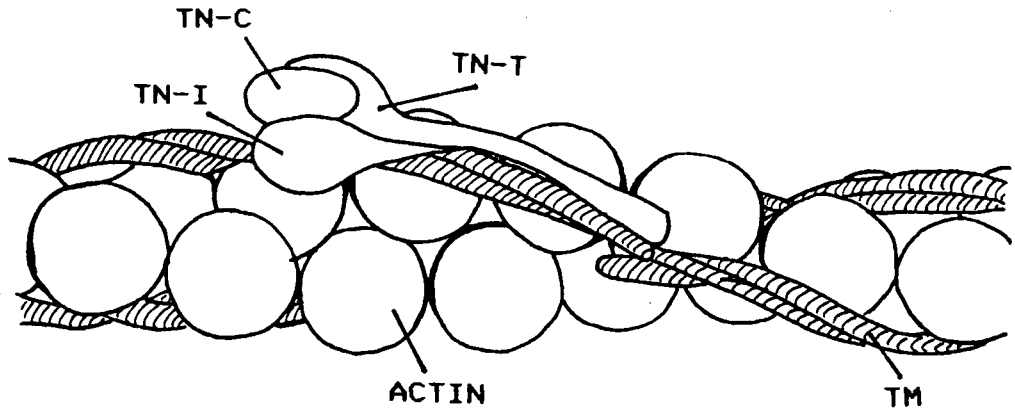

Figure 3: Schematic diagram of the proposed model of a thin filament of vertebrate striated muscle. Actin makes up the helical backbone of the structure with the TN complex consisting of TN-C, TN-I and TN-T (Côté, 1983).

The highly organised structure of actin in striated muscle contrasts with the dynamic nature of actin in non-muscle cells. Actin is the major component of microfilaments found in the cellular cytoskeleton. The cytoskeleton is a fibrous matrix of proteins which can span the cytoplasm of cells between the nucleus and the inner surface of the plasma membrane establishing cell shape and motility. The cytoskeleton often is particularly dense just below and parallel to the cell's plasma membrane. There are three distinct systems of filaments in the cytoskeleton: microfilaments (6-7nm diameter), intermediate filaments (7-

11nm diameter) and microtubules (22nm diameter). Figure 4 shows an immunofluorescence micrograph of actin filaments in a resting cell.

By controlling the assembly, stability and interactions of actin filaments, cells are able to regulate their shapes and positions, to shuttle their internal contents about and to exclude them from certain regions. Some of the diverse cellular activities that involve actin include cytoplasmic streaming, phagocytosis, cell division, the regulation of the distribution of certain membrane proteins and functional interconnection of the cell membrane with the nucleus (Korn, 1978).

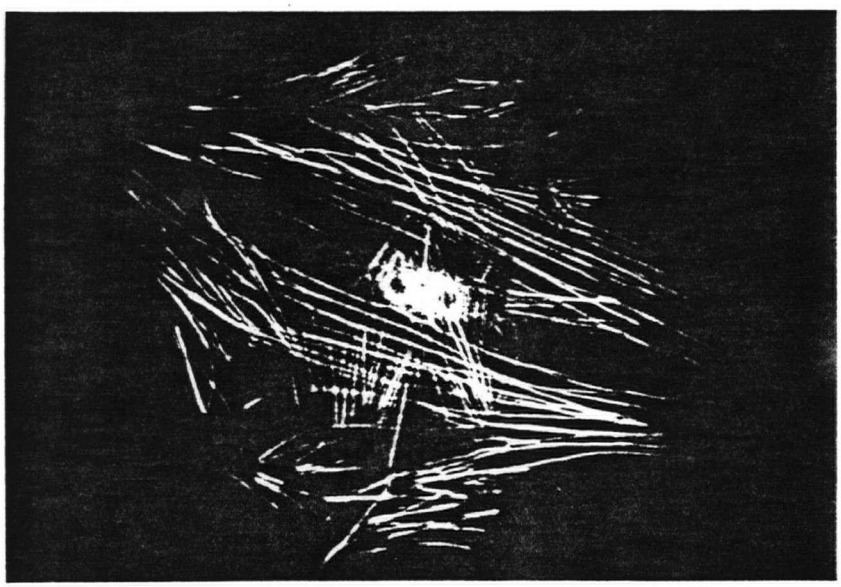

Figure 4: Immunofluorescence micrograph of actin filaments in a resting rat fibroblast (Stryer, 1981)

Non-muscle and muscle actins closely resemble each other in chemical composition, physical properties and physiological function (Korn, 1978).

1.1.4 Actin-binding Proteins

The formation of actin assemblies and their diversity, which allow many different functions, depends on the actions of a large repertoire of actin-binding proteins. These proteins are named according to the action they have on actin and are summarised in figure 5.

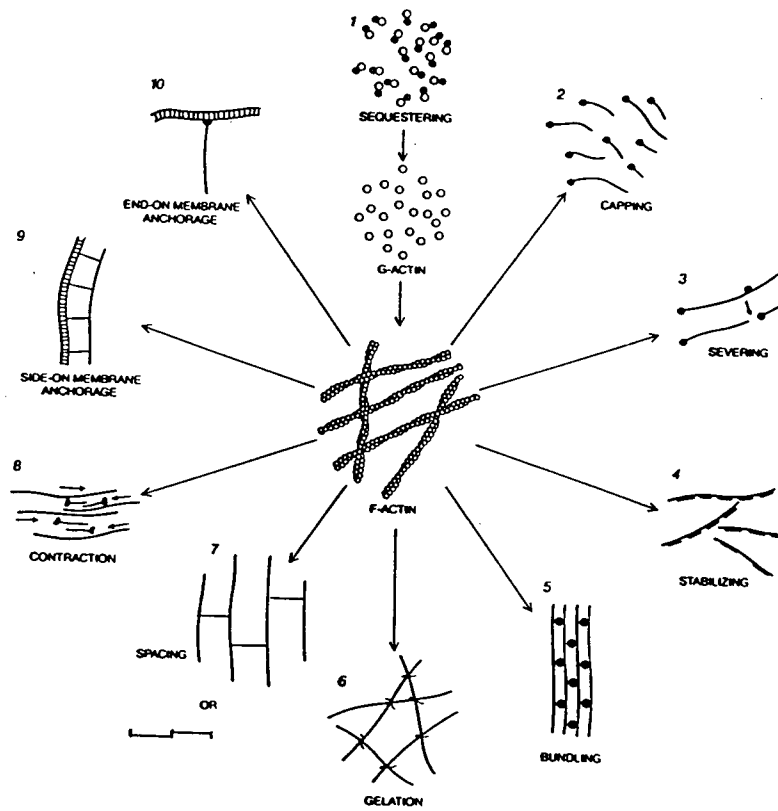

Figure 5: Summary of actin-binding proteins and a schematic representation of their effects on actin filaments or actin monomers (Pollard and Craig, 1982)

1.1.5. Introduction to Gelsolin

Gelsolin is representative of a class of actin-modulating proteins occurring widely, from lower eukaryotes to mammals, which have powerful effects on the length of actin filaments (Stossel et al., 1985). It was first discovered in rabbit lung macrophages and sera by Yin and Stossel in 1979. It was originally called 'actin depolymerizing protein' (ADP) and 'brevin' (from the Latin *brevis*, short) after it was found to shorten rather than depolymerize actin filaments. The name gelsolin comes from its ability to *sol*ate actin filament *gel*s (Noberg et al., 1979). It is unusual among mammalian proteins in that one form is produced for intrinsic intracellular use and another is made specifically for secretion (Yin et al., 1984). Cytoplasmic and plasma gelsolins are both globular proteins, with apparent molecular masses of about 90 kDa and 93 kDa, respectively, as assessed by polyacrylamide gel electrophoresis in the presence of sodium dodecyl sulphate (SDS-PAGE). The chemical similarity between cytoplasmic and plasma gelsolins, initially suggested on the basis of N-terminal protein sequence analysis (Yin et al., 1984), was comfirmed when the complete sequence of human gelsolin cDNA showed that cytoplasmic and plasma gelsolins were identical except for a 25 amino acid extension on the amino-terminal of the plasma variant. A single gene encodes two different mRNAs that specify the cytoplasmic and plasma forms (Kwiatkowski et al., 1986).

Horse plasma gelsolin resembles other plasma and cytoplasmic gelsolins in its physical and chemical properties (Ruiz Silva and Burtnick, 1990). Hydrodynamic calculations suggest a molecular mass of 75kDa, lower than the 90 kDa estimated from its mobility on SDS-PAGE and closer to 80.9 kDa calculated for pig plasma gelsolin from its amino acid sequence (Way and Weeds, 1988).

1.1.6. Interactions of Gelsolin with Actin

Gelsolin has three major interactions with actin. First, gelsolin accelerates the initial rate of salt-induced actin polymerization from actin monomers (nucleation activity). Second, gelsolin binds to the fast growing end of actin filaments and inhibits further elongation at that end (capping activity). Third, gelsolin has the ability to sever actin filaments by breaking the non-covalent bond between actin monomers (severing activity). The combined effect of these three interactions is to promote the formation of a large number of short actin filaments which are capped at their 'barbed' ends (Harris and Weeds, 1984). These effects are dependent on calcium concentrations (Bryan and Kurth, 1984). Gelsolin has two calcium binding sites and two actin binding sites and requires micromolar concentrations of calcium ions to bind any actins. On the removal of calcium, by chelation with EGTA, only one actin is removed from the ternary complex. The 1:1 actin/gelsolin complex that remains does not sever actin filaments but it does block the

'barbed' end of actin filaments with high affinity. Once gelsolin blocks the 'barbed' end of a filament, it can not be dissociated from actin by chelation of calcium.

Way et al. (1989) carried out studies on a number of mutant gelsolins to show that gelsolin was composed of six large segmental repeats of about 15,000 M_r and proposed a hypothesis to account for the properties of gelsolin (figure 6).

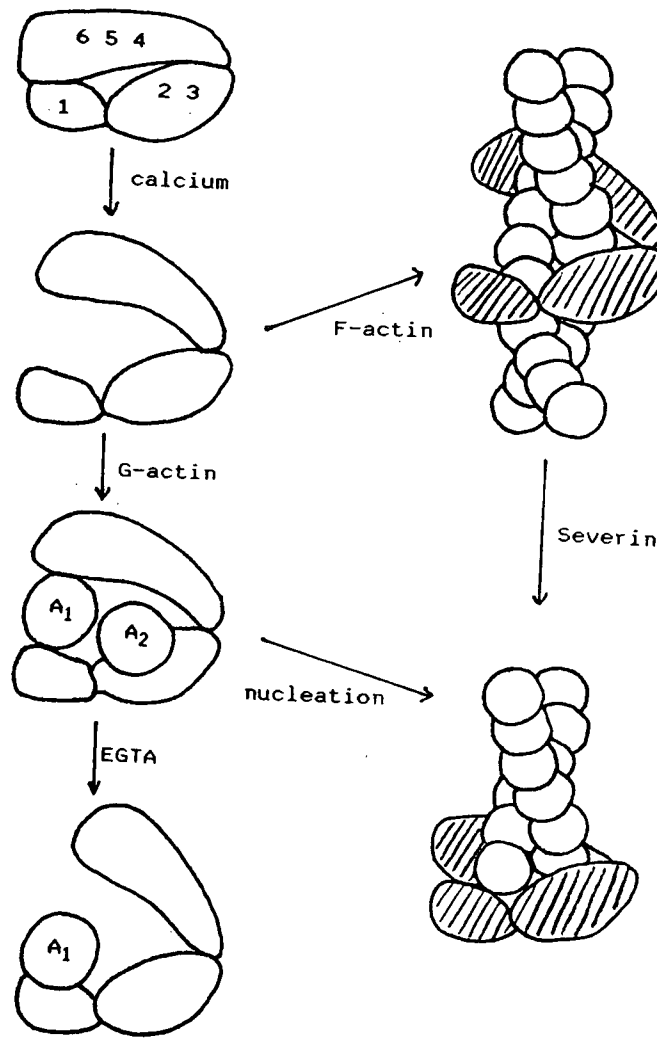

Figure 6: Schematic model to show the interaction of human plasma gelsolin with actin (Way et al., 1989).

This is a schematic model to show the interaction of gelsolin with actin. In the absence of calcium, actin binding is prevented by the close association of segment 1 and segments 4-6. Addition of calcium facilitates binding of two G-actin monomers, one to segments 2-3 and another initially to segments 4-6 but also to segment 1. (This ternary complex is the nucleating species under polymerizing conditions.) On removal of calcium, binding by segments 2-3 and 4-6 is lost, leaving a single monomer tightly associated with segment 1. In the presence of F-actin, gelsolin binds to the sides of filaments via segments 2-3 and both severing and capping occur by the interaction of segment 1 and probably segments 4-6 with an adjacent actin subunit. Way and coworkers also found similar segmental repeats in three other actin-binding proteins. The evidence suggests that these proteins constitute a family of proteins that has evolved from a precursor of about 130-150 amino acids (Way and Weeds, 1988).

1.1.7. Gelsolin and the Cytoskeleton

As gelsolin-actin interactions cannot be reversed completely by removal of calcium, a second agent is required to dissociate the gelsolin-actin complex. It has been proposed that the membrane phospholipid metabolites phosphatidylinositol 4,5-bis-phosphate (PIP_2) and phosphatidylinositol monophosphate (PIP) serve as such agents. They are able to dissociate gelsolin from small

actin complexes and capped filament ends (Janmey and Stossel, 1987).

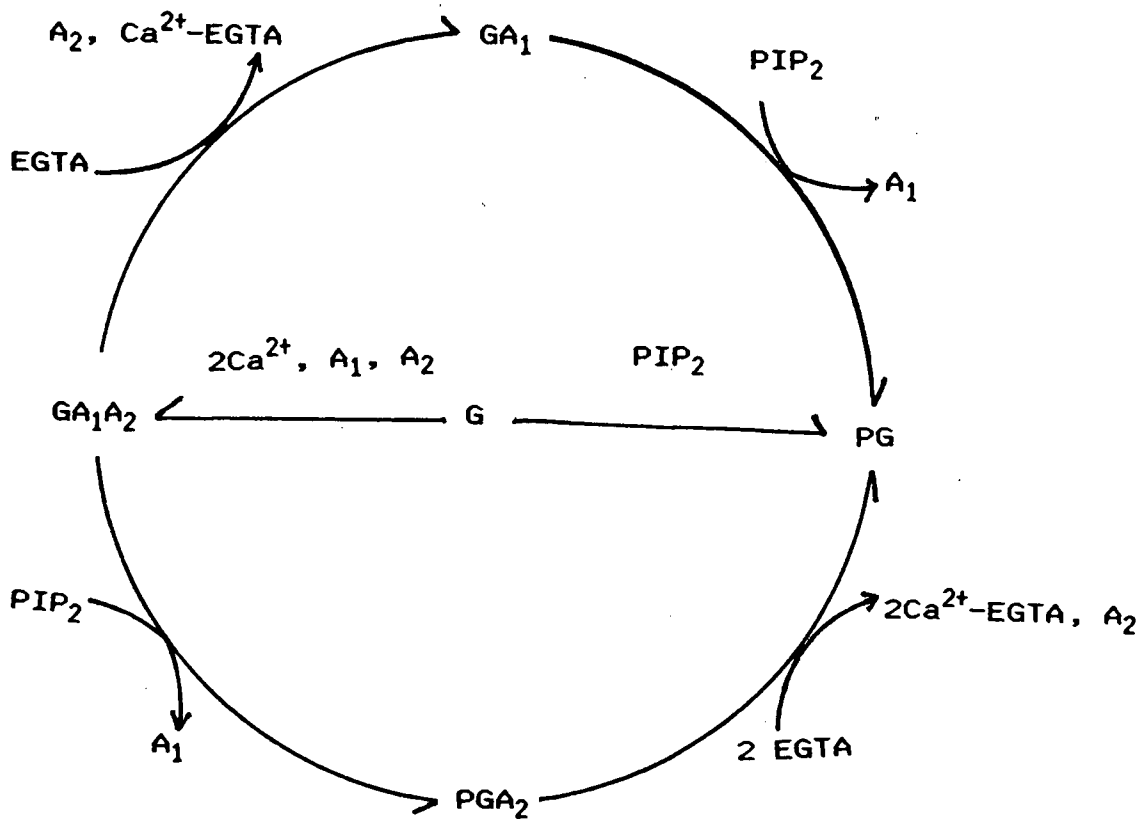

Figure 7: Summary of different gelsolin-actin complexes as regulated by Ca^{+2} and PIP_2. The binding of PIP_2 to gelsolin is unaffected by Ca^{+2} (Janmey et al., 1987).

Figure 7 is a summary of different gelsolin-actin complexes that are regulated by calcium and PIP_2/PIP. Gelsolin (G) binds 2 actin monomers (A_1 and A_2) in the presence of 2 calcium ions. Chelating the calcium with EGTA removes A_2, leaving a binary complex GA_1. A_1 can be dissociated by the

binding of PIP_2 or PIP to gelsolin, to give PG. The second route, binding PIP_2 before chelating calcium with EGTA, results in PG also.

1.1.8. Gelsolin in Plasma

The ionic conditions of plasma are ideal for actin polymerization, so that virtually all actin released into blood would be expected to polymerize. Actin may be released into blood as a result of tissue injury, disease, trauma or simply during normal cellular turnover. Even a small number of long actin filaments in plasma could have serious consequences. An increase in plasma viscosity could seriously impede blood flow. Also, cells circulating in the blood could become entrapped in the filaments (Lind et al., 1988). Actin filaments could themselves plug up capillaries (Kwiatkowski et al., 1988) and may interfere with other processes, such as blood clotting (Lind et al., 1986). Moreover, each actin monomer has a bound ADP, and ADP activates platelets (Scarborough et al., 1981), so extracellular actin could induce platelet aggregation.

Plasma gelsolin and vitamin D-binding protein (DBP) are the two major actin-binding proteins in mammalian blood. They serve to scavenge actin from plasma. Removal of actin proceeds in 2 stages. Firstly, plasma gelsolin nonproteolytically severs F-actin into short filaments that contribute little to plasma viscosity. Gelsolin remains tightly bound to one end of the shortened filaments.

Secondly, DBP, which binds with high affinity to actin monomers, causes a slow depolymerization of the short, gelsolin capped filaments (Janmey et al., 1987). DBP-actin complexes are rapidly removed from plasma by the liver.

PART 2: OPTICAL TECHNIQUES

1.2.1. Fluorescence Spectroscopy

The measurement most frequently performed on biological molecules is the absorption of visible or ultraviolet light. Absorption occurs in about 10^{-15} seconds and is governed by spin selection rules which allow only transitions between states of like multiplicity.

Light emission, on the other hand, can reveal molecular properties of biological molecules quite different from those revealed by light absorption. The process takes place on a much slower time-scale, typically 10^{-8} seconds for aromatic fluorophores, allowing a much wider range of interactions and perturbations to influence the spectrum. Since most organic chromophores have an even number of (paired) electrons, the transitions are between the ground state (S_0) and higher electronic states (S_1, S_2, etc.). As vibrational motion is on the 10^{-12} second timescale, the absorption process leaves the molecule in a vibrationally excited state (Franck-Condon principle). In solution, this excess vibrational energy is dissipated rapidly to the surrounding solvent via collisions, quickly relaxing the molecule to the lowest vibrational level of the first excited singlet state (S_1). Further deactivation to S_0 can occur by emission of a photon (fluorescence, rate constant k_f) or by competing non-radiative processes. The non-radiative processes (and the rate constants that characterise them) include internal conversion (k_{ic}),

intersystem crossing (k_{is}) and quenching (k_q). All of these processes compete directly to depopulate the excited singlet state. Therefore, the fraction of excited singlets that become de-excited through fluorescence (quantum yield, ϕ_f) is simply

$$\phi_f = k_f / (k_f + k_{ic} + k_{is} + k_q[Q])$$

where [Q] is the concentration of quencher molecules.

The absorption and emission of light can be illustrated by a Jablonski diagram (figure 8):

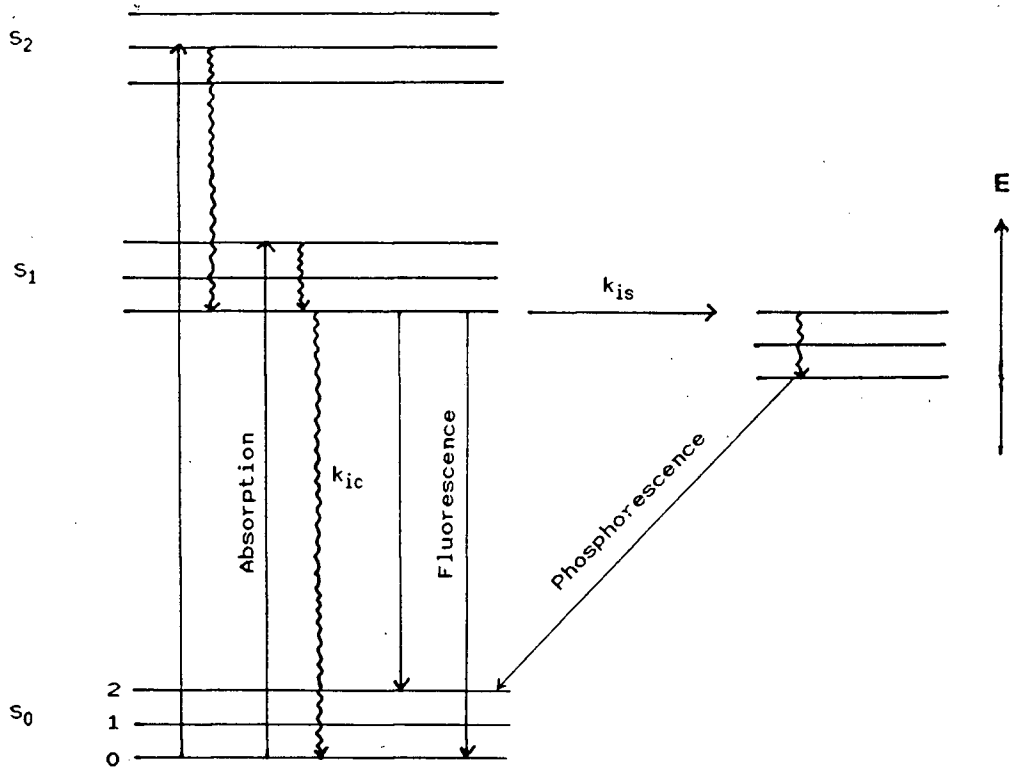

Figure 8: Schematic diagram for the process involved in electronic excitation and de-excitation of fluorescent molecules.

The ground, first and second electronic states are depicted by S_0, S_1, and S_2, respectively. At each of these

electronic energy levels, the fluorophore can exist in a number of vibrational energy levels depicted by 0, 1, 2, 3, etc.

The flourescence intensity, I(t) of a sample of fluorescent molecules at time t after turning off the source of excitation is given by

$$I(t) = I_0 \exp(-t/\tau_f)$$

where I_0 is the fluorescence intensity at time zero and the fluorescence lifetime, $\tau_f = (k_f + k_{ic} + k_{is} + k_q[Q])^{-1}$.

1.2.2. Fluorophores

Chromophores which display significant fluorescence (fluorophores) generally possess delocalised electrons formally present in conjugated double bonds.

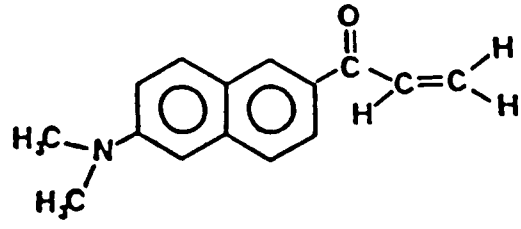

Figure 9: Thiol-specific fluorescent probe, acrylodan (Prendergast et al., 1983).

The fluorescent reagent, acrylodan, reacts specifically with thiol groups, such as occur on cysteine residues in proteins. It is highly sensitive to its environment

(Pendergast et al., 1983) and has proved useful in studies of tropomyosin (Clark and Burtnick, 1988).

1.2.3. Environmental Effects

Flourescence is generally much more sensitive to the environment of a fluorophore than is light absorption. Therefore, fluorescence is an effective technique for following interactions among proteins and conformational changes in them.

1.2.3.1. Solvent Relaxation

The emission from fluorophores generally occurs at wavelengths longer than those of light absorption (figure 10). This loss of energy between absorption and emission of light, the Stokes' shift, is a result of several dynamic processes, including vibrational relaxation. The use of polar solvents, such as water, will cause considerable relaxation of the excited state of the fluorophore, which generally has a higher dipole moment than the ground state. This would reduce the energy gap between the excited and ground states, causing emission to be red-shifted relative to absorption. The rate constants k_{ic} and k_{is} are enhanced in polar solvents, resulting in a decrease in fluorescence intensity.

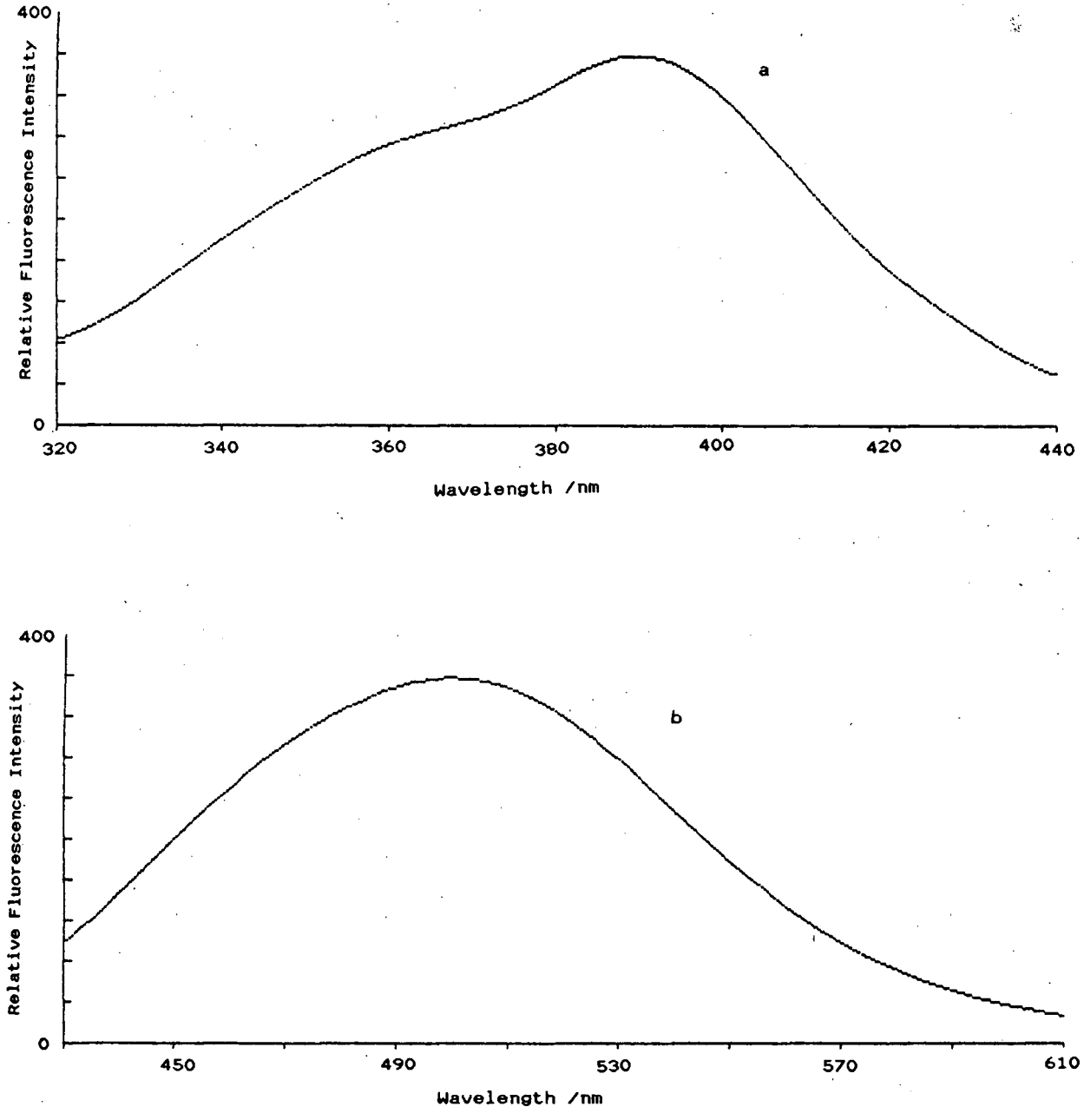

Figure 10: Excitation (a) and emission (b) spectra of acrylodan-labelled gelsolin. Emission wavelength was 497nm in (a).Excitation wavelength was 390nm in (b). Solution conditions were 150mM KCl, 25mM Tris-HCl, 1mM DTT and 1mM EGTA, pH 8.0 at 25^{0}C.

1.2.3.2. Quenching

Flourescence quenching involves any process which decreases the fluorescence quantum yield, ϕ_f. The rate of collisional quenching of fluorescence of a fluorophore bound to a protein by a quencher will be less than that of the fluorophore free in solution and will be reflected in a change in slope of a plot of F_0/F vs [Q] according to the Stern-Volmer equation:

$$F_0/F = 1 + k_q\tau_0[Q]$$

where F_0 and F are the fluorescence intensities in the absence and presence of quencher Q, τ_0 is the fluorescence lifetime of the molecule in the absence of Q and k_q is the bimolecular rate constant for quenching.

A wide variety of substances act as quenchers of fluorescence, one of which, I^-, was employed in studies described in this thesis. Quenching by this halogen is thought to be a result of intersystem crossing to an excited triplet state, promoted by spin-orbit coupling of the excited fluorophore and I^- (Kasha, 1952).

1.2.4. Fluorescence Polarisation

If plane-polarised light is used to excite a fluorescent system, and if linearly polarised components of the emission are detected, information can be obtained about the size,

shape and flexibility of the macromolecule to which the fluorophore is attached.

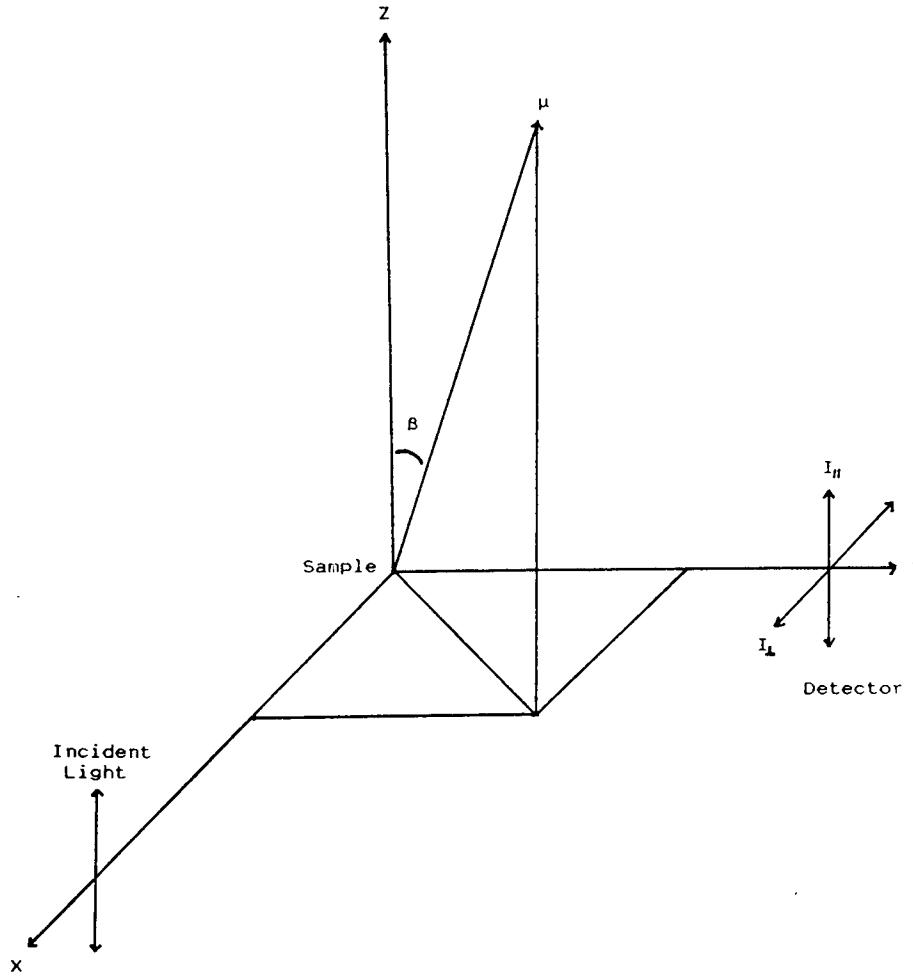

Figure 11: Diagramatic representation of excitation of a fluorescent molecule with vertically polarized light and subsequent detection of emission at 90^0 (Cantor and Schimmel, 1979).

This figure shows a typical arrangement for polarisation measurements where the incident light is parallel to the z axis and μ is the absorption dipole moment of the fluorescent species. The ability of μ to interact with vertically polarised light falls off with $\cos^2\beta$, producing a

set of excited molecules that is cylindrically symmetrical about the z axis. Polarisation (P) is defined by:

$$P = (I_{\parallel} - I_{\perp}) / (I_{\parallel} + I_{\perp})$$

where $I_{\parallel}$ and $I_{\perp}$, respectively, are intensity of emission parallel and perpendicular to the plane of polarisation of the excitation light.

For a completely rigid system, P = 0.5. This value is never found for fluorophores in solution. The measured values are smaller due to rotational diffusion and long fluorescence lifetimes.

By monitoring polarisation values, one can tell if the bound fluorescent probe is becoming more rigid or more mobile as a result of some perturbation to the system.

1.2.5. Circular Dichroism

Plane polarized light may be represented as the sum of two equally intense but oppositely handed circularly polarized components. If a sample absorbs one of the circularly polarised components more strongly than the other, the resultant light that emerges from the sample is elliptically polarised. This difference in absorption coefficient of the sample for left and right circularly polarized beams defines the circular dichroism, $\triangle\epsilon$, of the sample:

$$\Delta\epsilon = \epsilon_L - \epsilon_R$$

where ϵ_L and ϵ_R are, respectively, extinction coefficients for left and right circularly polarised light.

The production of an elliptically polarised beam has lead to circular dichroism being expressed in terms of the ellipticity, θ, of the ellipse that characterizes the light, where tan θ equals the ratio of the minor to the major axis of the ellipse. The molar ellipticity $[\theta]$, expressed in deg $cm^2 dmol^{-1}$, is given by

$$[\theta] = 3300\ (\epsilon_L - \epsilon_R)$$

A CD spectrum consists of a plot of $[\theta]$ vs wavelength. Molar ellipticity, $[\theta]$, can be calculated from observed ellipticity at a specific wavelength:

$$[\theta] = M\theta/10dc$$

where θ is the observed ellipticity (deg), M is the molar mass (g mol^{-1}), d is the cell pathlength (cm) and c is the concentration (g mL^{-1}). If M expresses the mean residue molar mass, then $[\theta]$ is called the mean residue (or residual) ellipticity.

Protein circular dichroism in the region of the spectrum between 190nm and 230nm is dominated by contributions from the peptide backbone. One can consider a protein to consist

of α-helix, β-sheet and random coil (more correctly, undefined) structures. Estimates of the fraction of amino acid residues in each of these types of conformation can be obtained from measured CD of the protein being studied. To calculate the fractional composition of secondary structure types, one could consider the following equation at 2 different wavelengths and use the constraint that

$f_\alpha + f_\beta + f_\gamma = 1$

$$[\theta] = f_\alpha X_\alpha + f_\beta X_\beta + f_\gamma X_\gamma$$

where X_α, X_β and X_γ are, respectively, the mean residue ellipticities of 100% pure α-helix, β-sheet and random coil proteins. These values can be estimated using CD spectra of homopolypeptides of known structure (Greenfield and Fasman, 1969) or by comparative analysis of the CD spectra of proteins of known three dimensional structure (by X-ray crystallography) (Saxena and Wetlaufer, 1971).

Protein denaturation can be followed using circular dichroism. The loss of CD signal between 210nm and 230nm on thermal denaturation is due to unfolding of α-helix and β-sheet structures into the random coil structure, which has a low CD signal in this spectral region.

2. MATERIALS AND METHODS

PART 1: PROTEINS

2.1. Purification of Actin

Actin was purified from an acetone powder of rabbit muscle tissue (Pel-Freez Biologicals) according to a modification of the method of Spudich and Watt (1971).

10g of acetone powder was dispersed (at 4°C) in 200mL of 2mM Tris-HCl, 0.2mM $CaCl_2$, 0.2mM ATP, 1.0mM DTT, pH 8.0 (Buffer A) for 30 minutes. The mixture was filtered through a double layer of cheesecloth. The residue was washed with 100mL of buffer A and filtered again before being discarded. Both filtrates were combined and filtered through Whatman #1 filter paper and centrifuged at 80,000 xg for 1 hour. After discarding the pellet, KCl (to 50mM) and $MgCl_2$ (to 2mM) were added to the supernatant and the actin was allowed to polymerise (without stirring) at room temperature for 2 hours. Solid KCl then was added to 0.8M and the solution was stirred gently for 1.5 hours. It then was centrifuged at 80,000 xg for 3 hours. The supernatant was discarded. The F-actin pellet was resuspended in 30mL of buffer A and converted to G-actin by dialysing at 4°C for 3 days, changing to fresh buffer A every 24 hours. The G-actin was clarified by centrifugation at 80,000 xg for 3 hours and stored in buffer A.

The concentration of G-actin was measured spectrophotometrically using an absorption coefficient at 290nm of 0.63 mL $mg^{-1}cm^{-1}$ (Porte and Harricane, 1986).

2.2.1 Purification of Gelsolin

Gelsolin was purified from frozen horse blood plasma by a modification of the methods of Bryan (1988) and Ito, et al. (1990).

During the thawing process 100µL each of leupeptin and pepstatin (stock solutions at 2 mg mL^{-1} in water and DMSO, respectively) were added to 1L of plasma along with PMSF to 0.2mM. The thawed plasma was dialysed at 4°C against 4 changes, 10 volumes per change, of 25mM Tris-HCl, 0.5mM $CaCl_2$ and 1mM NaN_3, pH 7.5, and centrifuged at 10,000 xg for 10 minutes to remove aggregated material. Solid NaCl was added to the supernatant to 35mM.

The plasma then was mixed with 4L of DEAE Sephadex A-50 ion exchanger (Pharmacia) that had been equilibrated against 50mM NaCl, 25mM Tris-HCl, 0.5mM $CaCl_2$, 1mM NaN_3, pH 7.5. This batch procedure was carried out at 4°C with occasional, gentle stirring for approximately 2 hours. The slurry then was filtered and the ion exchanger was washed with buffer. At this stage the plasma lost its characteristic yellow colour to the ion exchanger and the filtrate was colourless.

To the filtrate (total volume between 2.1L and 2.5L), EDTA and NaN_3 were added to 10mM and 1mM, respectively, and the pH was adjusted to 7.8.

This solution was applied to a 36x6 cm column of DEAE-Sephadex A-50 ion exchanger previously equilibrated at 4^0C in 50mM NaCl, 25mM Tris-HCl, 1mM EDTA, 1mM NaN_3, pH 7.8. After washing the column with the equilibrating buffer (2 bed volumes), proteins were eluted with a 0.05M to 0.3M NaCl gradient and collected in 25mL fractions. Those fractions containing gelsolin were pooled and concentrated by ultrafiltration to 2.5-3.0 mg mL^{-1} using an Amicon YM30 membrane. No precipitation was observed, in contrast to reports that, at concentrations greater than 1 mg mL^{-1}, pig plasma gelsolin was unstable in solution (Weeds et al., 1986).

These concentrated solutions were dialysed at 4^0C against 2 changes of 25mM Tris-HCl, 1mM EDTA, 1mM PMSF, pH 8.0 (Buffer I) for 24 hours. The dialysed solution was applied at 4^0C to a 2.5x17 cm Affi-Gel Blue (immobilised cibacron Blue F3GA gel) column equilibrated with buffer I. The column then was washed with 2 bed volumes of buffer I and gelsolin was eluted with buffer I containing 1mM ATP and collected in 2mL fractions. These fractions were concentrated by ultracentrifugation using an Amicon YM30 membrane.

Concentrations of horse plasma gelsolin were measured spectrophotometrically using an absorption coefficient at 280nm of 1.4 mL $mg^{-1}cm^{-1}$ (Ruiz Silva and Burtnick, 1990).

2.2.2 Determination of Purity

The purity was checked at various stages of the preparation of gelsolin by electophoresis on 10% polyacrylamide gels (BioRad Mini-Protean II System) in the presence of sodium dodecyl sulphate (SDS) and 2-mercaptoethanol (LaemmLi, 1970). Phosphorylase b (Sigma) was used as a standard. Pure gelsolin produced a single band with a relative molecular mass of 90,000.

2.2.3 Determination of Activity

Actin-severing activity of gelsolin was measured by viscometry. Aliquots of gelsolin containing solutions were added to 50µM actin solutions in 150mM KCl, 25mM Tris-HCl, 2mM $CaCl_2$, 1mM $MgCl_2$, 0.1mM ATP, and 1mM DTT, pH 8.0. Measurements were made in a Cannon-Manning semi-micro viscometer (size 100) at 27°C. A volume of 1mL was required to fill the viscometer, which had a flow time of 102s for buffer.

2.2.4 Fluorescent labelling of Gelsolin.

Gelsolin initially was dialysed against 1L of 150mM KCl, 25mM Tris-HCl, 1mM EDTA and 1mM DTT, pH 8.0 at 4°C for 24 hours. DTT was removed prior to labelling by dialysis in the above buffer without DTT for a further 4 hours.

Acrylodan (Molecular Probes) was dissolved in 100µL of *N,N*-dimethylformamide (DMF) and added directly to the gelsolin sample until an approximate 20x molar excess of

acrylodan to protein had been achieved. The reaction was allowed to proceed overnight in the dark at $4^{0}C$ on a mechanical rocker. The gelsolin/acrylodan mixture was dialysed against 1L of 150mM KCl, 30mM Tris-HCl, 1mM EGTA, and 1mM DTT, pH 8.0 for 4 hours and centrifuged at 15,000 xg for 15 minutes to remove the unreacted acrylodan. The acrylodan-labelled gelsolin (ACRG) was dialysed further against the above buffer for 3 days, changing the buffer on the second and third days. ACRG produced a single fluorescent band on a 10% SDS-PAGE gel.

2.2.5 Degree of Labelling

The average number of acrylodan molecules per gelsolin molecule (degree of labelling) was measured by independent determination of acrylodan and protein concentrations in an ACRG solution. Acrylodan was analysed spectrophotometrically using a molar absorption coefficient of 12900 $M^{-1}cm^{-1}$ at 360nm. The concentration of labelled gelsolin in ACRG solution was measured using the BioRad microassay procedure based on the observation that the absorbance maximum of a dye (Coomassie Brilliant Blue G-250) shifts from 465nm to 595nm when binding to protein occurs (Bradford, 1976). Unlabelled gelsolin (of known concentration) in the presence of dye was used to plot a standard curve of concentration vs absorbance at 595nm. The concentration of gelsolin in an ACRG solution was interpolated from the standard curve. For a given ACRG solution:

$$\text{Degree of labelling} = \frac{[\text{Acrylodan}]}{[\text{Gelsolin}]}$$

The degree of labelling was found to be 1.9 ± 0.5 acrylodans per gelsolin based on 6 labelling experiments.

2.2.6 Summary of Gelsolin Purification

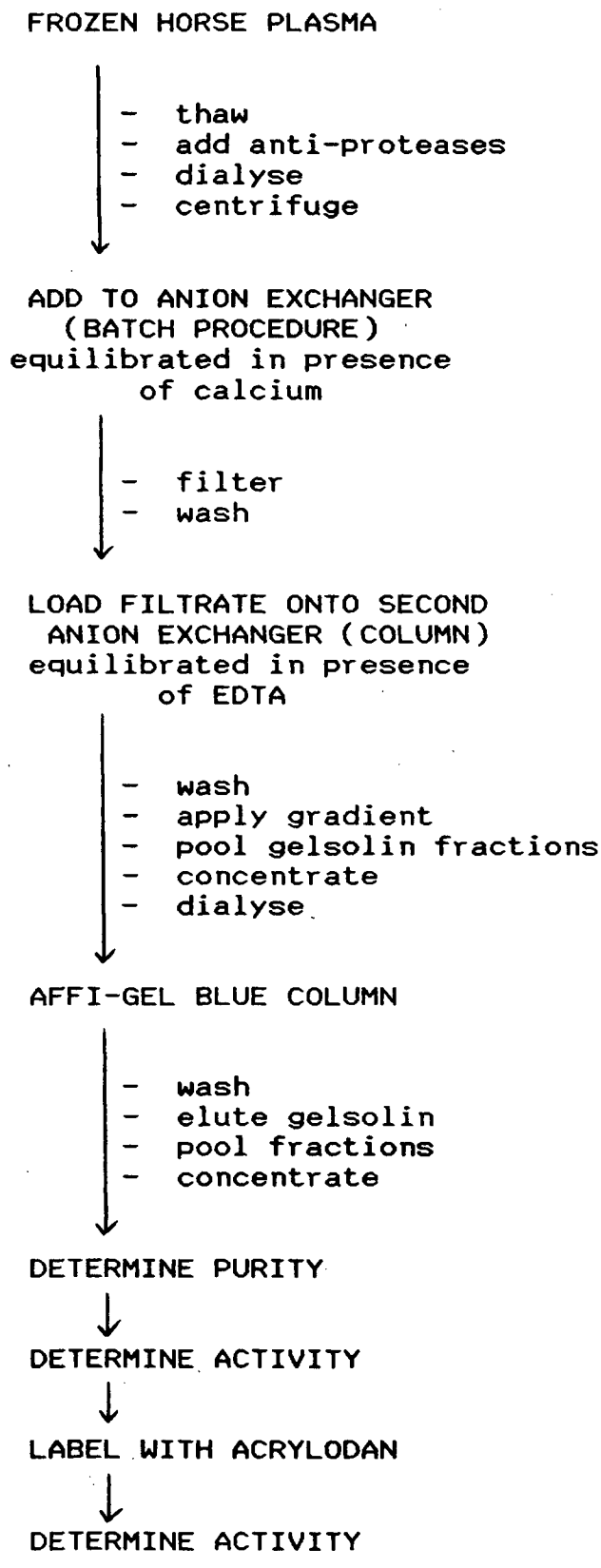

PART 2: OPTICAL TECHNIQUES

2.3.1 Absorbance Measurements

A Lambda 4B UV/Vis Spectrophotometer (Perkin-Elmer) was used to detect proteins and measure concentrations at various stages during and after the purification procedure.

2.3.2 Flourescence Measurements

An LS-5B Luminescence Spectrometer equipped with a 7500 Series computer (Perkin-Elmer) was used for fluorescence studies. The excitation and emission wavelengths were 390nm and 497nm, respectively, with both excitation and emission slits set at 10nm band widths. Polarisation values were obtained by incorporating a semi-automatic polarisation accessory and using PTPOL software (Perkin-Elmer). The cell holder was thermostatically controlled for temperature studies.

2.3.3 Circular Dichroism

A rebuilt J-20 Automatic Recording Spectro-Polarimeter (Jasco) was used for recording circular dichroism measurements. The cell chamber was thermostatically controlled and purged with nitrogen. Thermal denaturation studies were performed at a fixed wavelength of 215nm. The output was standardized using D-Pantolactone (12mg in 100mL H_2O), which has an ellipticity of -17.3×10^3 deg cm^2dmol^{-1} at 220nm (Tuzimura et al., 1977). Thermal equilibration was

assessed to take between 10 and 15 minutes when monitored with a thermocouple in a cuvet in the sample chamber. Correlation of sample and bath temperatures in this way enabled all temperatures quoted in the text that follows to be reported as sample temperatures.

3. RESULTS AND DISCUSSION

PART 1: EFFECT OF CALCIUM ON ACRG

3.1.1. Labelling Gelsolin with Acrylodan

The degree of labelling of gelsolin with acrylodan was found to be 1.9 ± 0.5 acrylodans per gelsolin molecule, based on 6 labelling experiments. All ACRGs showed a single fluorescent band and then a single Coomassie blue-stained band on SDS-PAGE gels. This demonstrates the covalent binding of the acrylodan to gelsolin and that the reaction conditions have not resulted in cleavage of peptide bonds.

On excitation at 390nm, ACRG is highly fluorescent, showing a broad emission band with a maximum near 497nm (figure 10). The emission maximum is blue-shifted relative to 540nm for an acrylodan-mercaptoethanol adduct (Prendergast et al., 1983), 518nm for acrylodan-labelled tropomyosin (Clark and Burtnick, 1988) and 510nm for acrylodan-labelled DBP (Robinson, 1990). The emission maximum of ACRG is similar to those of acrylodan-labelled papain (491nm), parvalbumin (498nm) and carbonic anhydrase (501nm) (Prendergast et al., 1983) and suggests the environment of acrylodan on gelsolin to have considerable hydrophobic character.

A viscosity experiment was carried out to determine whether or not incorporation of the acrylodan label significantly affected the function of gelsolin with respect to its actin-severing ability (Table I).

TABLE I: VISCOSITY MEASUREMENTS ON ACRG

	Sample	Relative Viscosity
1.	Buffer A	1.00
2.	F-actin	1.53
3.	Gelsolin-actin	1.08
4.	ACRG-actin	1.09

Each sample (1mL volume) contained 150mM KCl, 25mM Tris-HCl, 2mM $CaCl_2$, 1mM $MgCl_2$, 1mM DTT and 0.1mM ATP, pH 8.0, at 27°C. Actin (1.2µM) was added to samples 2, 3, 4 and allowed to polymerize and equlibrate for 20 minutes. Gelsolin and ACRG were added to samples 3 and 4, respectively, to 0.92µM. Relative viscosities were calculated from the flow time of sample divided by the flow time of buffer A.

These values demonstrate that, under the conditions employed, ACRG is just as capable of severing actin filaments as is unlabelled gelsolin.

An additional experiment was carried out to investigate the possible effect on the degree of labelling of calcium ions. Identical samples were prepared by dialysis against 150mM KCl, 25mM Tris-HCl, 1mM DTT and 1mM EGTA, pH 8.0. One sample subsequently was dialysed against the same buffer containing 1mM $CaCl_2$ instead of EGTA. The labelling reaction was carried out as usual. Although the degree of labelling was found to be 2.3 in the presence of calcium and 1.6 in its absence, these values fell within the range of values

obtained previously, so no significance could be attached to the difference.

3.1.2 CD Studies on ACRG

Comparison of the CD spectra of ACRG labelled in the presence or absence of calcium with that of unlabelled gelsolin over the region from 210 to 245nm showed no significant differences (typical spectra are shown in figure 12). This suggests that neither incorporation of the label nor the presence or absence of Ca^{2+} during labelling produced a change in the conformation of the gelsolin molecule. These spectra resemble in shape and intensity those presented by Doi et al. (1990) for pig plasma gelsolin, except that we were not able to detect the small decrease in ellipticity they reported to be induced by addition of Ca^{2+} to their samples.

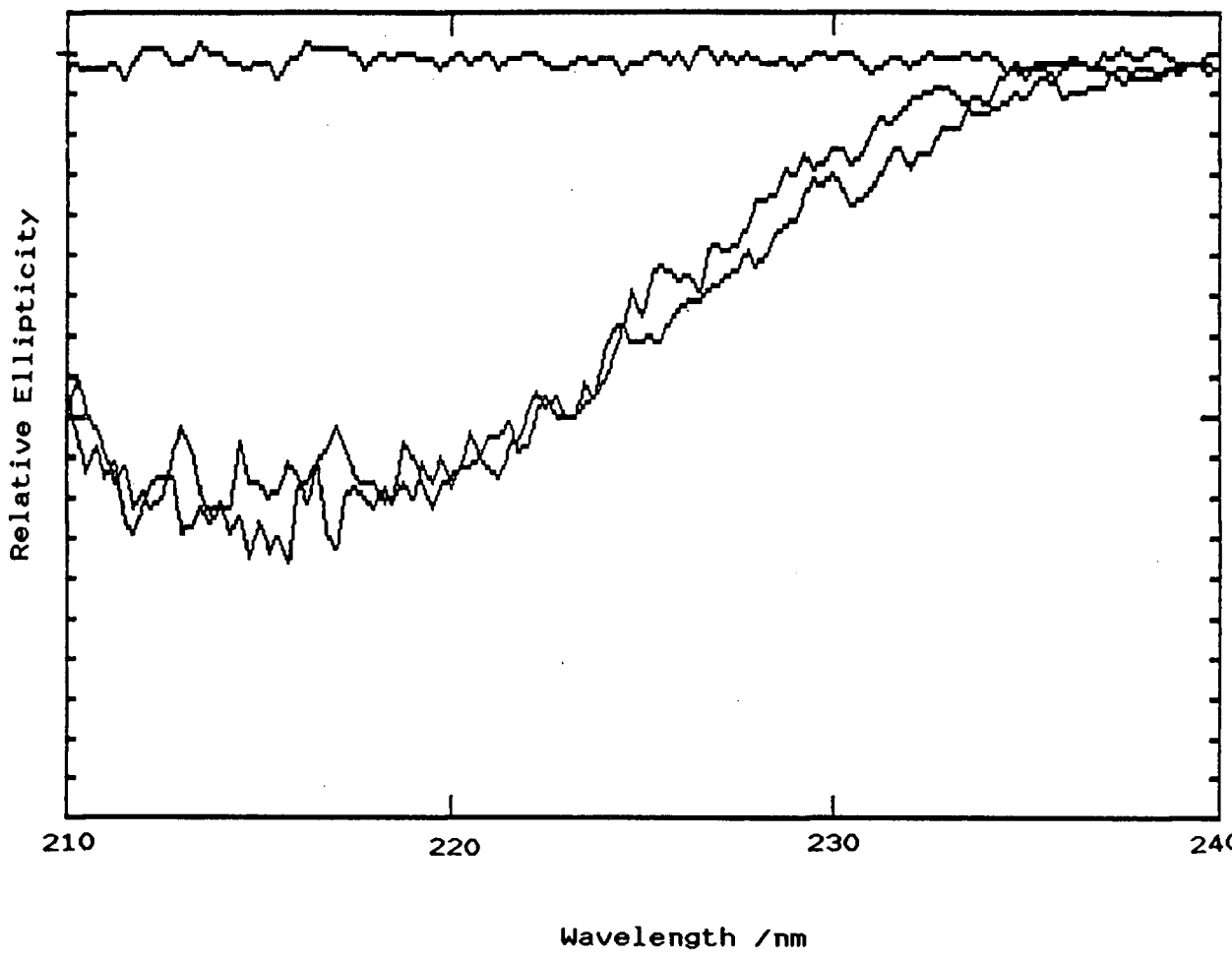

Figure 12: CD spectra of ACRG (labelled in the presence of excess EGTA) in the presence and absence of Ca^{2+}. Solution conditions were 150mM KCl, 25mM Tris-HCl, 1mM DTT and either 1mM EGTA or 1mM $CaCl_2$, pH 8.0. ACRG was present in each sample at 1µM in a 0.1 mm pathlength cell and the temperature was 10°C. The top spectrum is that for the EGTA-containing buffer. The lower spectra are not distinguishable statistically.

A comparison was made of the thermal stabilities of ACRG labelled in the presence of Ca^{2+}, ACRG labelled in EGTA and unlabelled gelsolin. The ellipticities at 215nm for each of the three proteins were observed at various temperatures in the presence and absence of Ca^{2+}. In each case, the gelsolin or ACRG was quite stable up to about 40°C. Subsequently, ellipticity values dropped dramatically. The EGTA-containing samples showed a melting transition centred at 48°C (figure 13). The Ca^{2+} containing samples were somewhat more stable, losing structure near 52°C (figure 14). At about 2°C above the melting temperature, a visible, irreversible precipitate appeared in all samples. Figure 15 compares the melting curves of gelsolin in the presence and absence of Ca^{2+}. Similar comparisons are made for the labelled proteins in figures 16 and 17. The slight stabilization afforded by Ca^{2+} is evident in each case.

3.1.3 Effect of Calcium on the Emission Spectrum of ACRG

Figure 18 illustrates the effect of calcium on the emission spectrum of ACRG. ACRG was dialysed against 150mM KCl, 25mM Tris-HCl, 1mM DTT and 1mM EGTA, pH 8.0. $CaCl_2$ (0.1M stock solution) was added to 2mM, so that a 1mM excess of Ca^{2+} over EGTA existed in the solution. The spectrum at 25°C was recorded 5 minutes after the addition of $CaCl_2$. To correct for dilution effects, a control experiment was carried out simultaneously in which an equal volume of

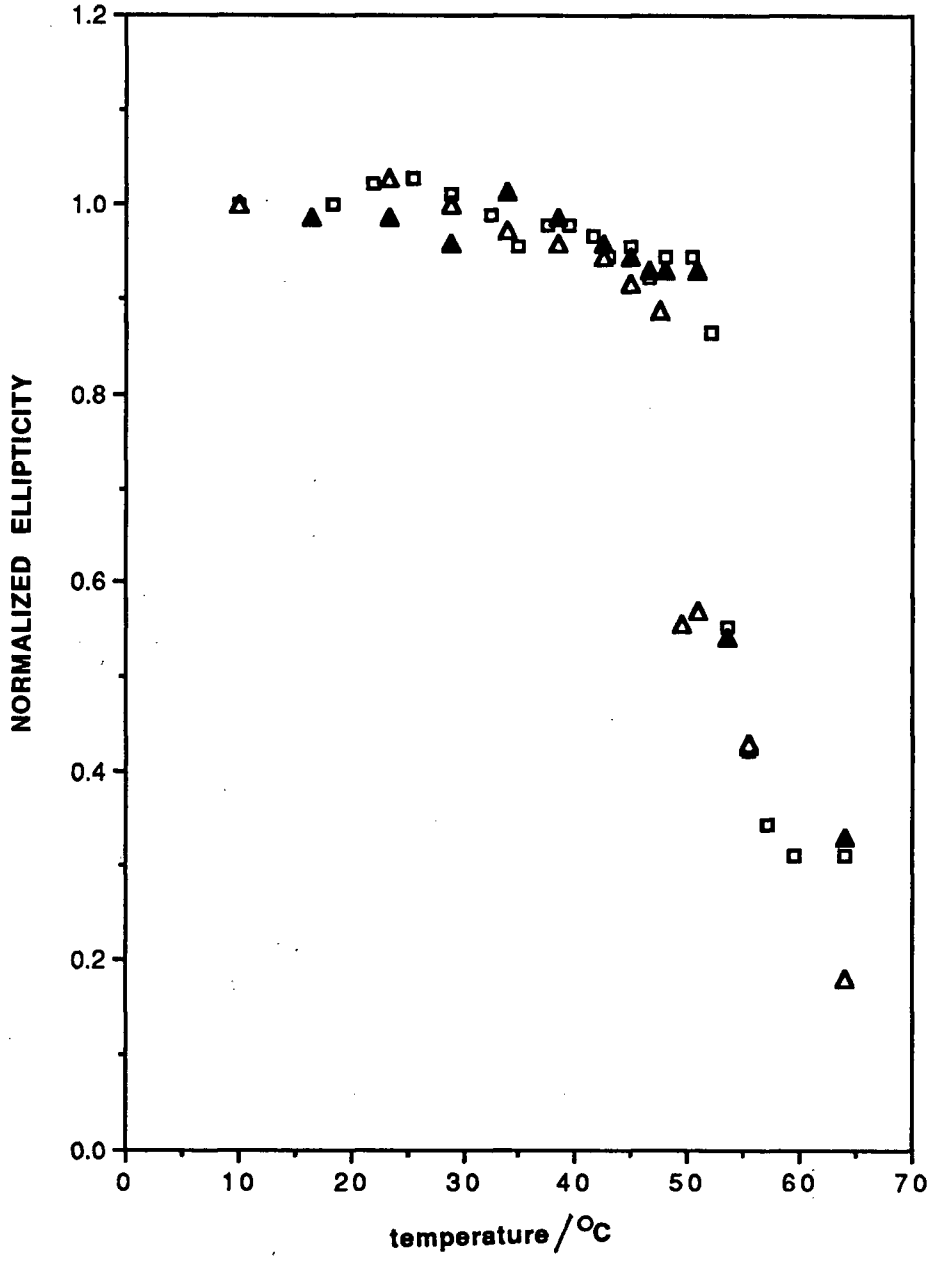

Figure 13 Change in normalized ellipticities of ACRG labelled in Ca^{2+} (▲), ACRG labelled in EGTA (Δ), and unlabelled gelsolin (□) with temperature. Solution conditions were 150mM KCl, 25mM Tris-HCl, 1mM DTT and 1mM $CaCl_2$, pH 8.0. CD was followed at 215nm. A 20 minute equilibration period was allowed subsequent to each change in temperature.

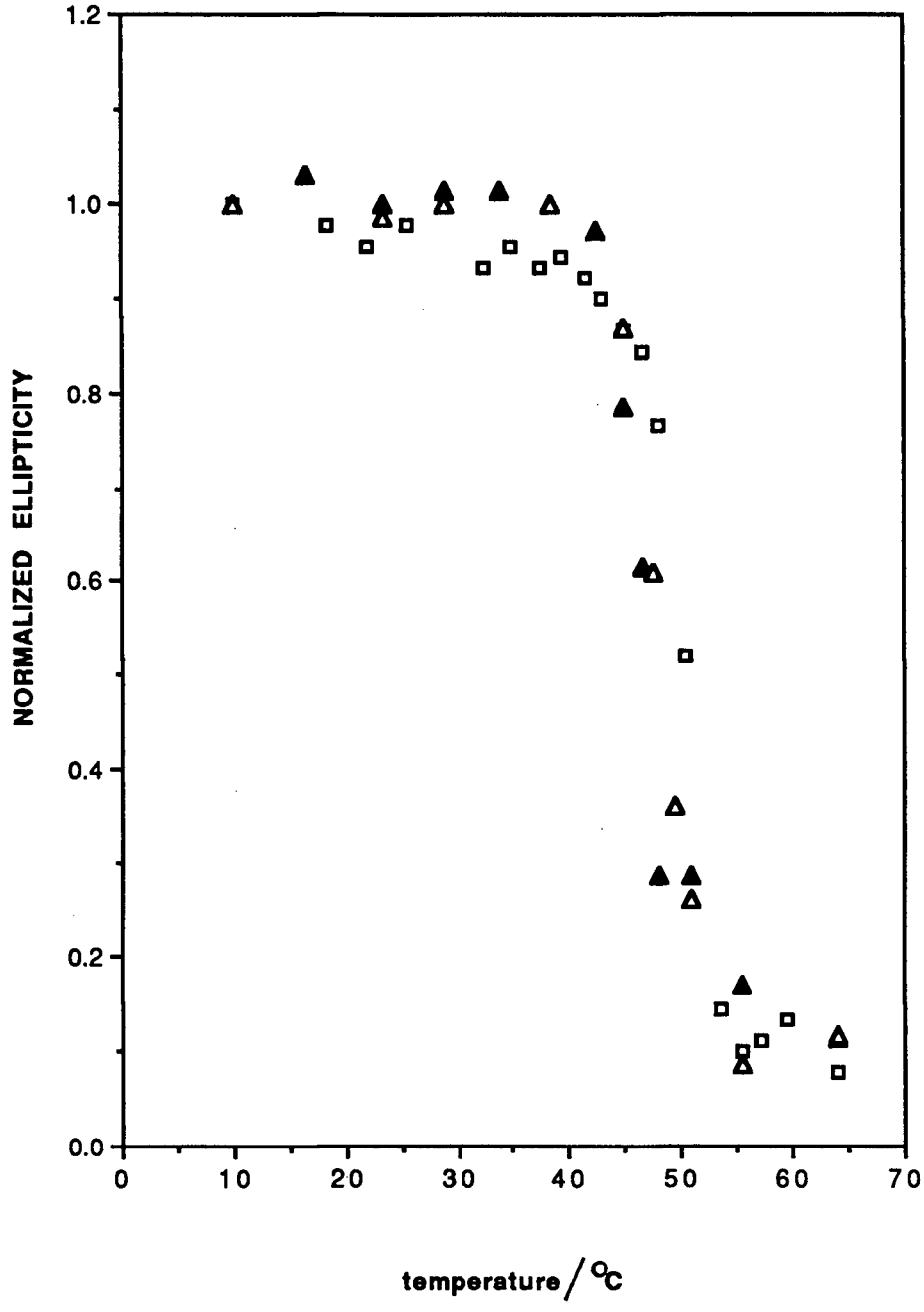

Figure 14 Change in normalized ellipticities of ACRG labelled in Ca^{2+} (▲), ACRG labelled in EGTA (△), and unlabelled gelsolin (□) with temperature. Solution conditions were 150mM KCl, 25mM Tris-HCl, 1mM DTT and 1mM EGTA, pH 8.0. CD was followed at 215nm. A 20 minute equilibration period was allowed subsequent to each change in temperature.

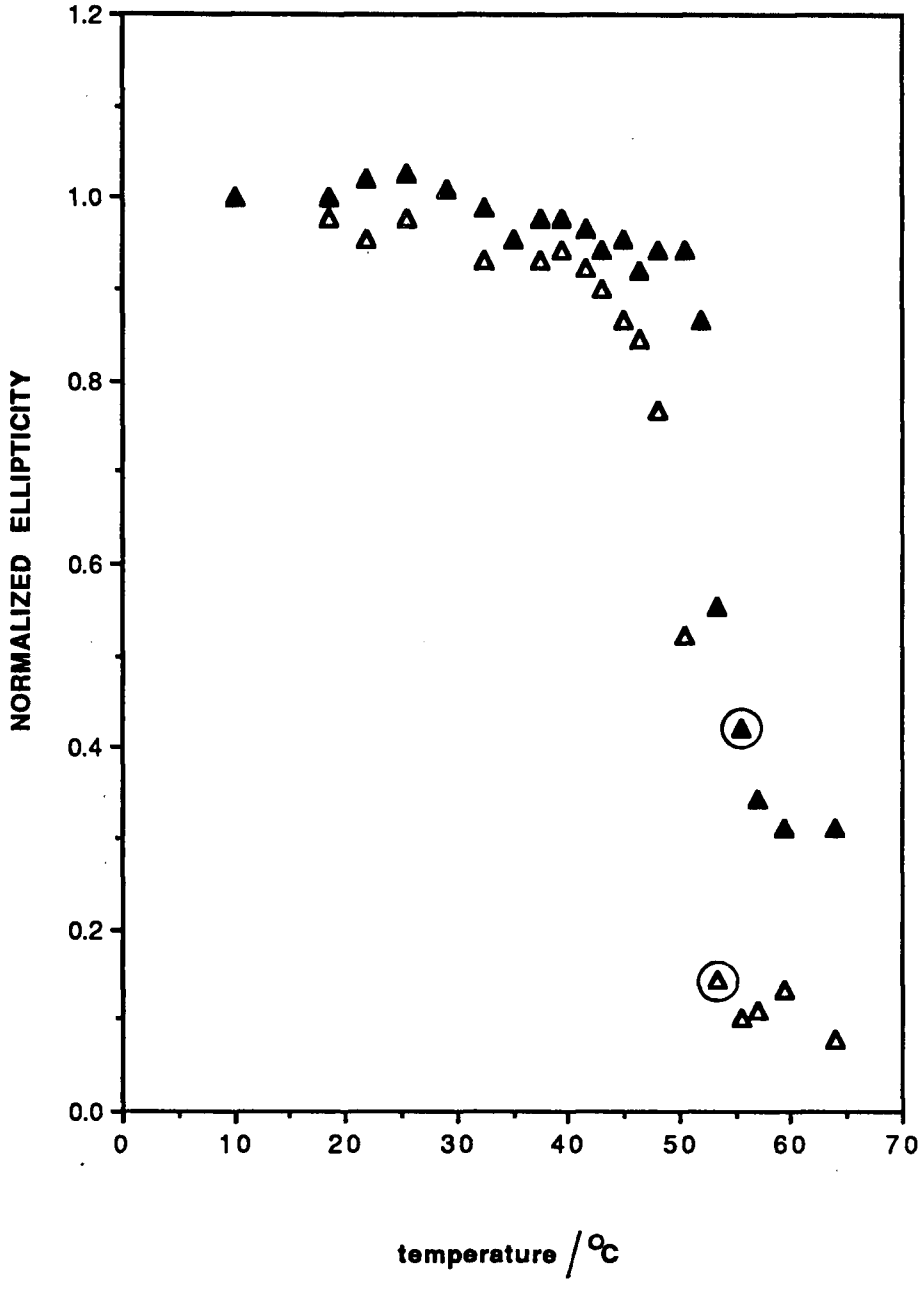

Figure 15 Change in normalized ellipticities of unlabelled gelsolin in the presence and absence of Ca^{2+} with temperature. Solution conditions were 150mM KCl, 25mM Tris-HCl, 1mM DTT and either 1mM Ca^{2+} (▲) or 1mM EGTA (△),pH 8.0. Circled points indicate onset of precipitation. CD was followed at 215nm. A 20 minute equilibration period was allowed subsequent to each change in temperature.

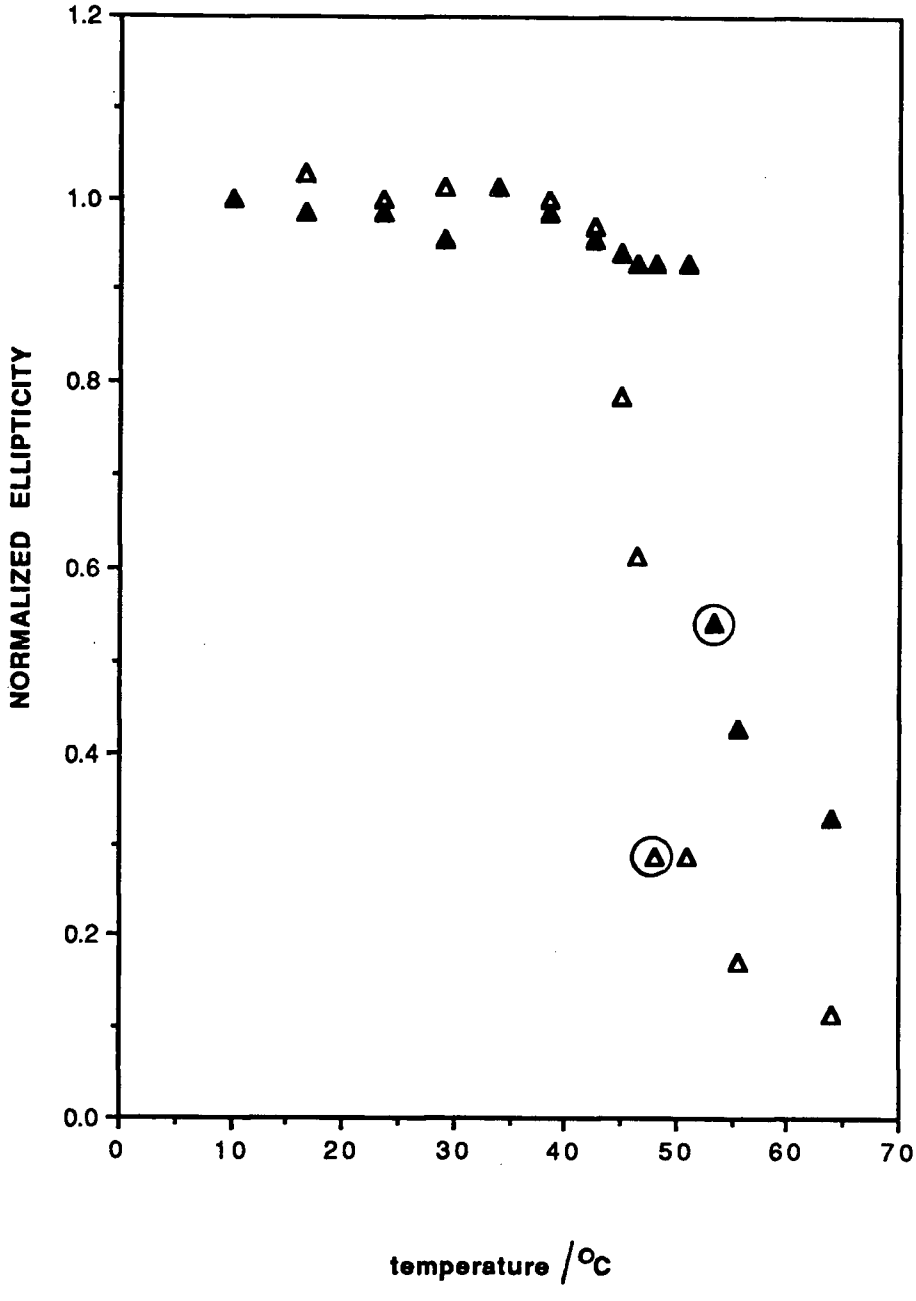

Figure 16 Change in normalized ellipticities of ACRG (labelled in presence of Ca^{2+}) in the presence and absence of Ca^{2+} with temperature. Solution conditions were 150mM KCl, 25mM Tris-HCl, 1mM DTT and either 1mM Ca^{2+} (▲) or 1mM EGTA (△), pH 8.0. Circled points indicate the onset of precipitation. CD was followed at 215nm. 20 minute equilibration period was allowed subsequent to each change in temperature.

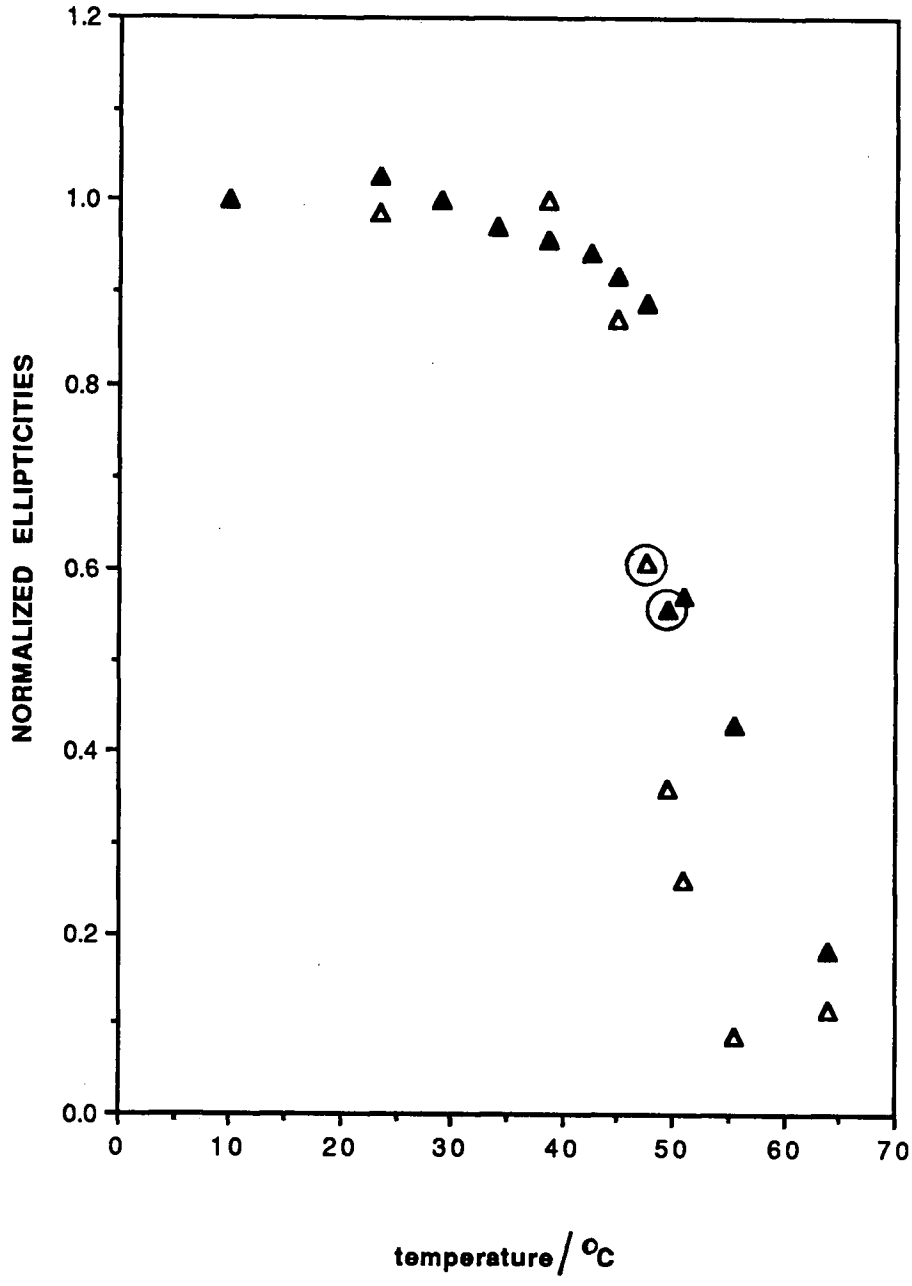

Figure 17 Melting curve of ACRG (labelled in absence of Ca^{2+}) in the presence and absence of Ca^{2+}. Solution conditions were 150mM KCl, 25mM Tris-HCl, 1mM DTT and either 1mM Ca^{2+} (▲) or 1mM EGTA (△), pH 8.0. Circled points indicate onset of precipitation. CD was followed at 215nm. A 20 minute equilibration period was allowed subsequent to each change in temperature.

distilled water was added to the protein solution in place of $CaCl_2$. There is a decrease in fluorescence with a slight red shift. This suggests that a conformational change in the protein, induced by calcium binding, is increasing the exposure of the probe to the solvent. This process is fully reversable by chelating the calcium ions with EGTA, indicating that the effect is due solely to the action of calcium ions.

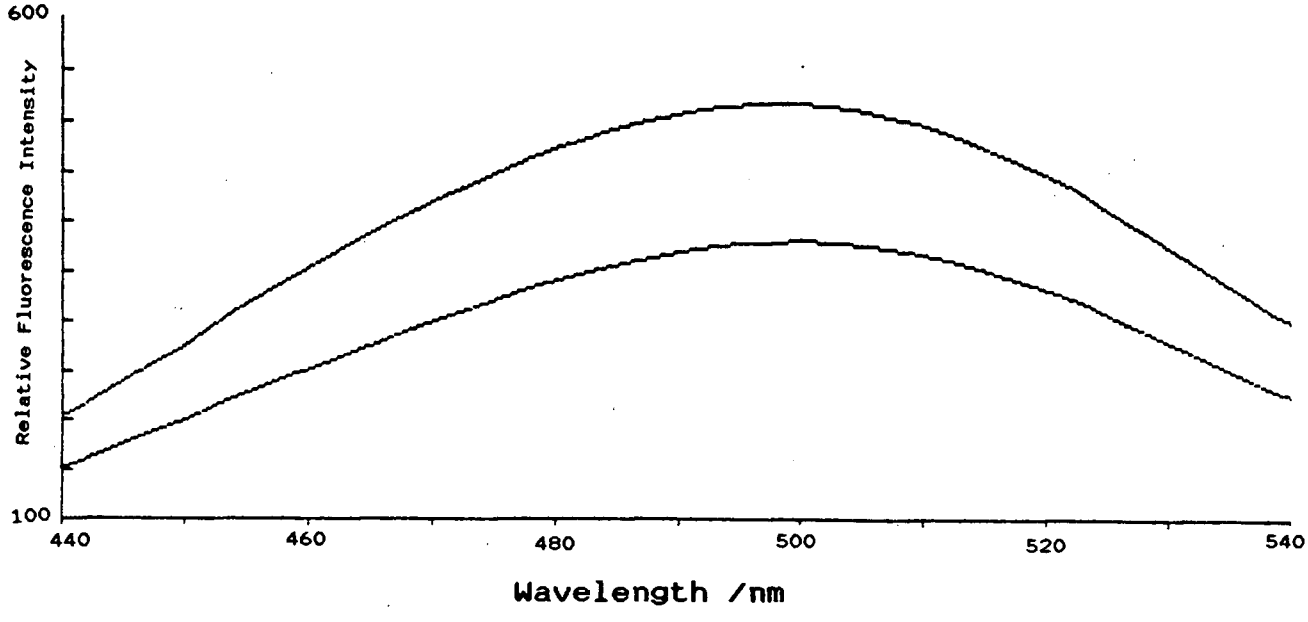

Figure 18: Effect of calcium on the emission spectrum of ACRG. The upper curve is the emission spectrum of ACRG (1µM) in the presence of 1mM EGTA. The lower curve is the spectrum 5 minutes after the addition of Ca^{2+} to 2mM. The excitation wavelength was 390nm. Initial solution conditions were 150mM KCl, 25mM Tris-HCl, 1mM DTT, 1mM EGTA, pH 8.0, at 25^{0}C.

3.1.4 Fluorescence Quenching Studies on ACRG

Increased exposure of the acrylodan probe to solvent in the presence of Ca^{2+} was confirmed by quenching studies. Figure 19 is a Stern-Volmer plot for iodide quenching of ACRG fluorescence. ACRG (1μM) was dialysed in 150mM KCl, 25mM Tris-HCl, 1mM DTT, pH 8.0, and either 1mM Ca^{2+} or 1mM EGTA. Two identical solutions were required for each plot, one to which KI was added and one to which was added equal molar amounts of KCl. These solutions, respectively, gave F and F_0 for each addition. This protocol simultaneously served to control for the effects of dilution and increased ionic strength. The steeper slope of the plot for the sample in the presence of Ca^{2+} reflects increased susceptibility of the probe to quenching under those conditions.

In an attempt to increase the accessability to I^- in the solvent, ACRG was denatured using 6M Gu-HCl. Figure 20 presents Stern-Volmer plots for iodide quenching of intact ACRG in the presence of calcium and for ACRG denatured with 6M Gu-HCl. The slopes of these plots are very similar. This suggests that the acrylodan probe in the presence of calcium is essentially as exposed to solvent as it is in the denatured protein.

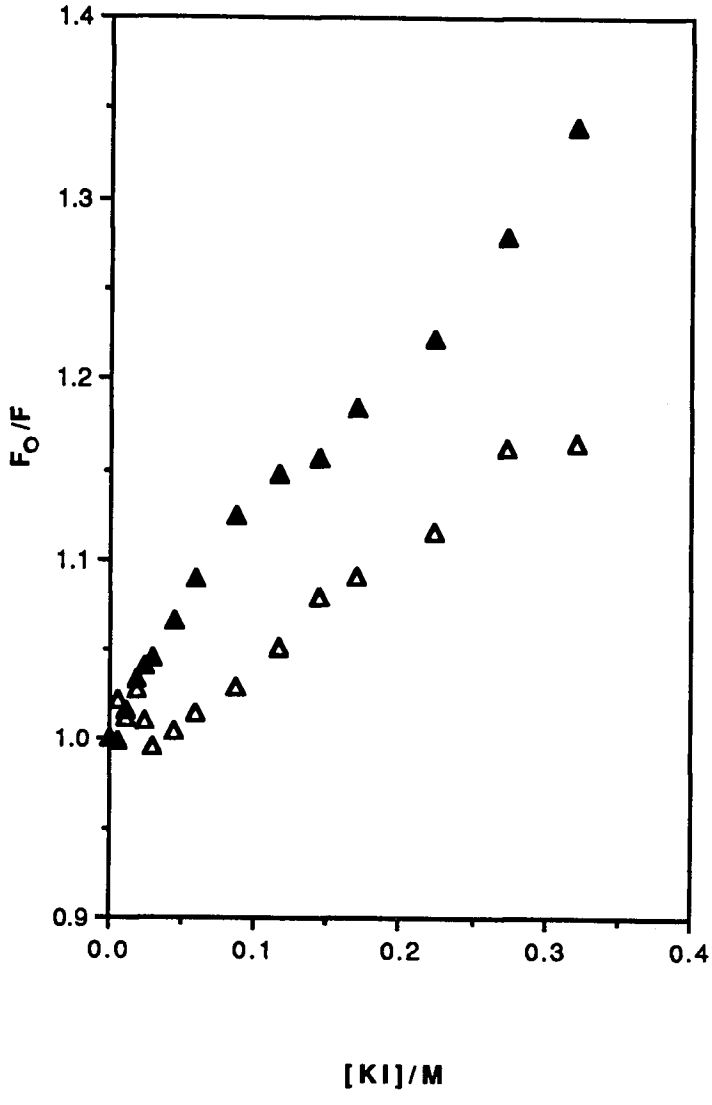

Figure 19: Stern-Volmer plots for iodide quenching of ACRG. One sample initially contained 0.25µM ACRG in 150mM KCl, 25mM Tris-HCl, 1mM DTT and 1mM EGTA, pH 8.0, at 25°C (△). The second sample was identical but contained 2mM $CaCl_2$ as well (▲). Excitation was 390nm and emission was 497nm in both cases.

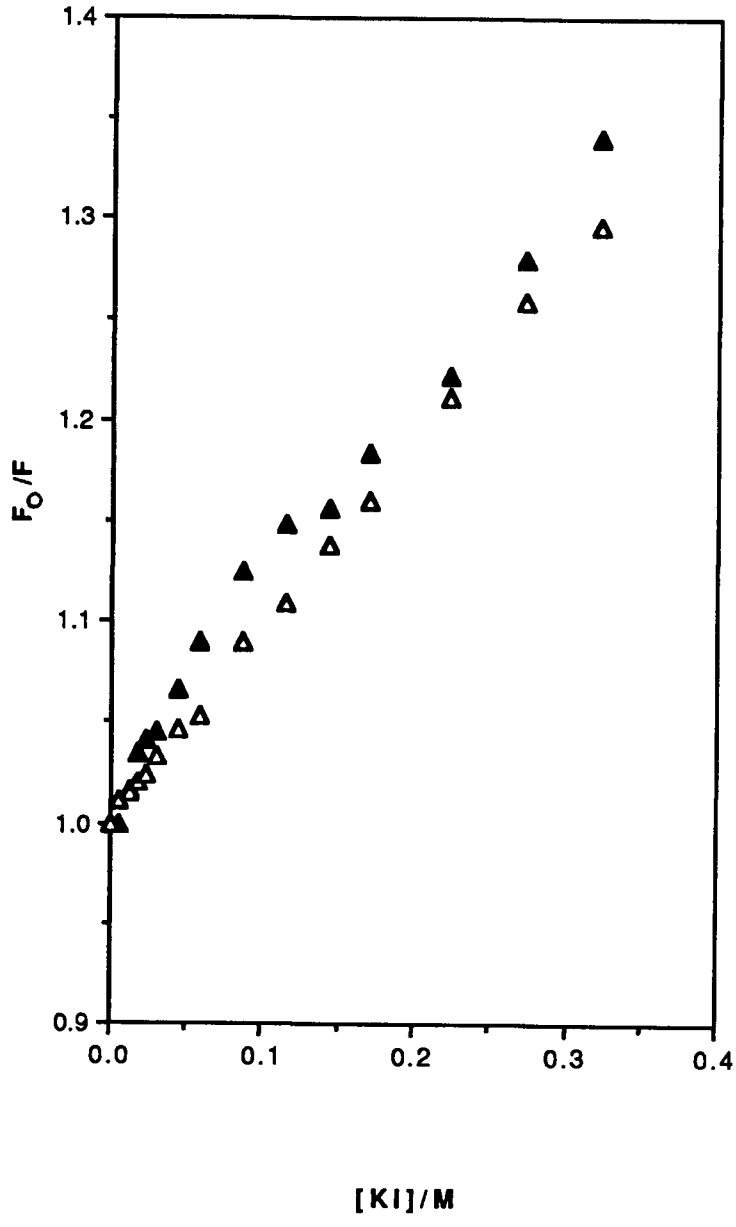

Figure 20: Stern-Volmer plots for iodide quenching of ACRG solutions. The Gu-HCl data (△) were collected from samples that initially contained 0.25μM ACRG in the presence of 6M Gu-HCl. The $+Ca^{2+}$ data (▲) are same as presented in figure 19. Excitation wavelength was 390nm and emission wavelength was 497nm in both cases.

3.1.5 Fluorescence Polarisation Studies on ACRG

Fluorescence polarisation was measured during thermal denaturation of ACRG in the presence and absence of calcium (figure 21). Two solutions were dialysed against 150mM KCl, 25mM Tris-HCl, 1mM DTT, pH 8.0, and either 1mM Ca^{2+} or 1mM EGTA.

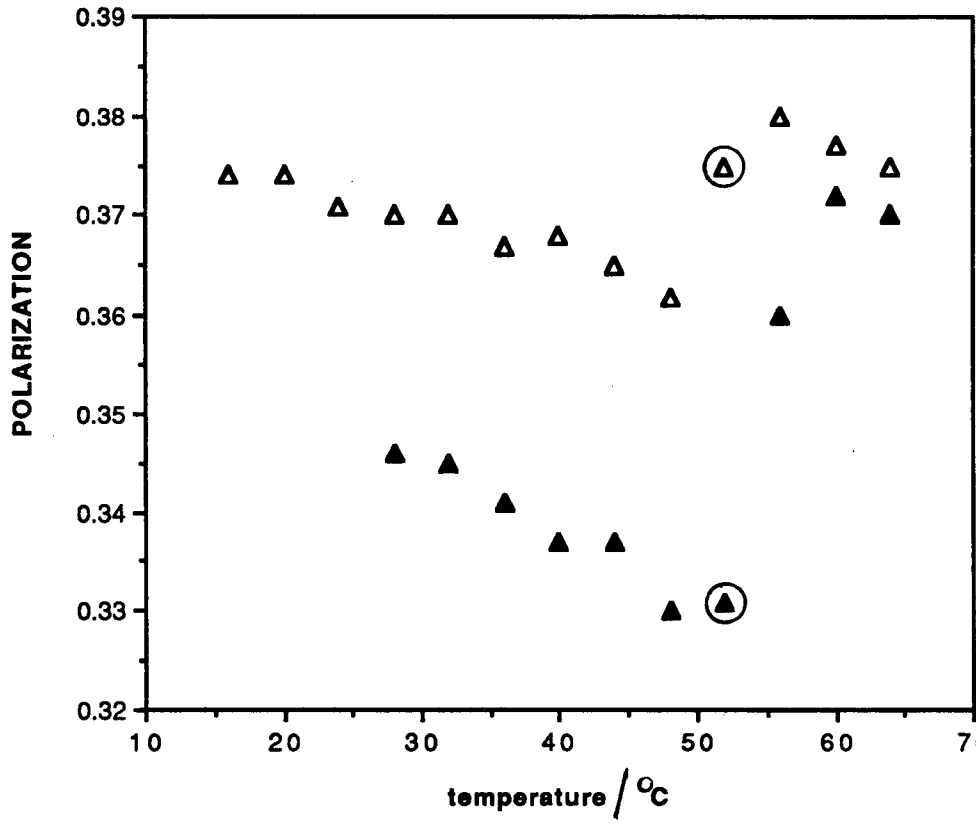

Figure 21: Fluorescence polarisation changes in ACRG (1µM) with temperature. Each polarisation value was the average of 3 measurements and typical standard deviations were ± 0.003. Solution conditions were 150mM KCl, 25mM Tris-HCl, 1mM DTT, pH 8.0, and either 1mM EGTA (△) or 1mM $CaCl_2$ (▲). Circled points indicate onset of precipitation. Excitation wavelength was at 390nm and emission wavelength at 497nm.

The steady decrease in polarisation value to about 50°C suggests a loss of gelsolin structural rigidity in the region of the acrylodan probe. The rigidity of the region is minimal at 48°C in 1mM EGTA and near to 50°C in 1mM Ca^{2+}. The sharp upward turn in each plot coincides with the onset of aggregation leading to irreversible precipitation. The consistently lower polarisation values found for ACRG in the presence of Ca^{2+} relative to in its absence are consistent with a model in which Ca^{2+} binding exposes the segment of polypeptide chain containing the acrylodan label to solvent.

PART 2: ACTIN BINDING TO ACRG

3.2.1 Effect of Actin on Emission Maximum of ACRG

Figure 22 illustrates the change in intensity of the fluorescence at 497nm for ACRG on titration with actin. Two samples were studied each initially containing ACRG (1μM), 150mM KCl, 25mM Tris-HCl, 1mM DTT and 1mM EGTA, pH 8.0 and one sample contained 2mM $CaCl_2$. Dilution effects were corrected for by multiplication of the intensity of each sample by the ratio of the sample volume to its initial volume.

Both samples show a steady drop in emission intensity on the addition of actin, suggesting an interaction between ACRG and actin that quenches acrylodan fluorescence. The effects of actin are independent of Ca^{2+}, in apparent

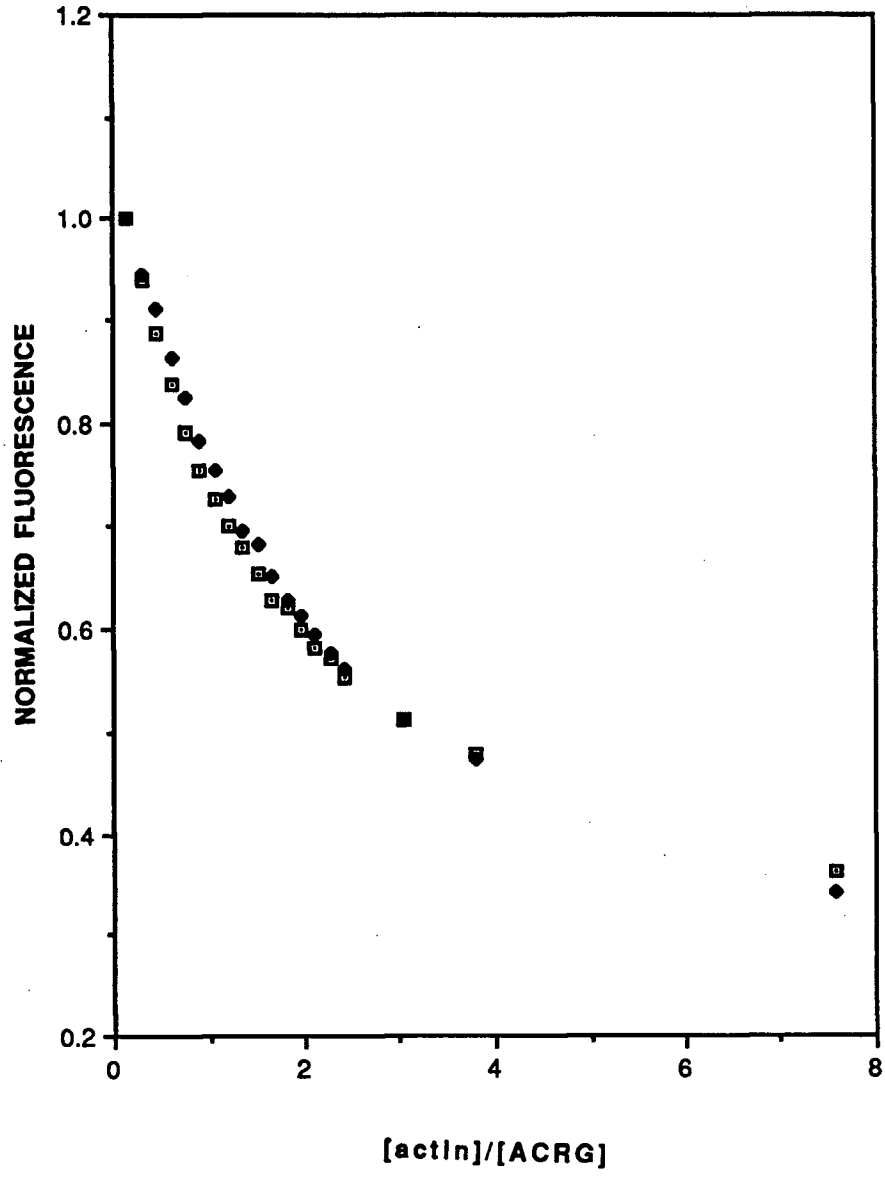

Figure 22: Changes in fluorescence intensity of ACRG on the binding of actin. One sample initially contained 1μM ACRG in 150mM KCl, 25mM Tris-HCl, 1mM DTT, 1mM EGTA, pH 8.0, at 25°C (▫). The other sample was identical but contained 2mM $CaCl_2$ as well (•). Excitation wavelength was at 390nm and emission was at 497nm. Normalization was achieved by dividing all readings by the appropriate sample fluorescence intensity in the absence of actin.

contradiction of the model of Way et al. (1988). The model suggests that actin should not interact with gelsolin in the absence of Ca^{2+}. One explanation of actin binding in the absence of Ca^{2+} might be that horse plasma gelsolin does not display Ca^{2+}-sensitive actin-binding. This compares with pig plasma gelsolin, which has been shown to interact with actin both in the presence and absence of Ca^{2+} (Harris and Weeds, 1983). Indeed, Ca^{2+}-dependent and Ca^{2+}-independent forms of this gelsolin have been separated by affinity chromatography on actin-Sepharose columns (Pope and Weeds, 1986). Plasma has a consistently high free Ca^{2+} concentration (about 1mM) and Ca^{2+}-sensitivity of a plasma protein function would be irrelevant. Another possible explanation comes from work by Pope et al. (1989). Their results showed irreversible loss of Ca^{2+}-sensitivity of gelsolin with respect to actin filament severing and actin monomer binding may be associated with the presence of Ca^{2+} during preparation and storage. The first stage of our purification of horse plasma gelsolin involves dialysis in a buffer containing 0.5mM Ca^{2+}. At this stage, one or more as yet unidentified plasma components may act to reduce the Ca^{2+}-sensitivity of gelsolin by some unknown mechanism.

In addition to indicating actin binding, the drop in fluorescence in figure 22 suggests that acrylodan is becoming more exposed to the solvent on interaction of ACRG with actin.

3.2.2 Quenching Studies of Actin-Gelsolin Complexes

Quenching studies were carried out on various actin-ACRG complexes to determine the exposure of the acrylodan probe to the solvent on the binding of actin. Two identical solutions were required for each plot, one to which was added aliquots of KI and the other to which was added equal amounts of KCl. These solutions, respectively, gave F and F_0 for each addition. Figure 23 presents a comparison of the iodide quenching of 11:1, 2:1 and 1:1 actin:ACRG complexes with ACRG alone.

Linear regression analysis of the curves in figure 25 gave the slopes and standard deviations shown in Table II:

TABLE II: IODIDE QUENCHING OF ACRG-ACTIN COMPLEXES

Actin:ACRG Complex	Slope/M^{-1}		S.D.
0:1	0.781	±	0.015
1:1	0.892	±	0.042
2:1	0.846	±	0.024
11:1	0.840	±	0.022

These results show that the slopes for the actin-ACRG complexes are higher than that for ACRG alone, but are statistically indistinguishable from each other. This suggests that the binding of actin to ACRG causes a slightly

increased exposure of the probe to I^- in the solvent, in agreement with the fluorescence drop induced by actin-binding.

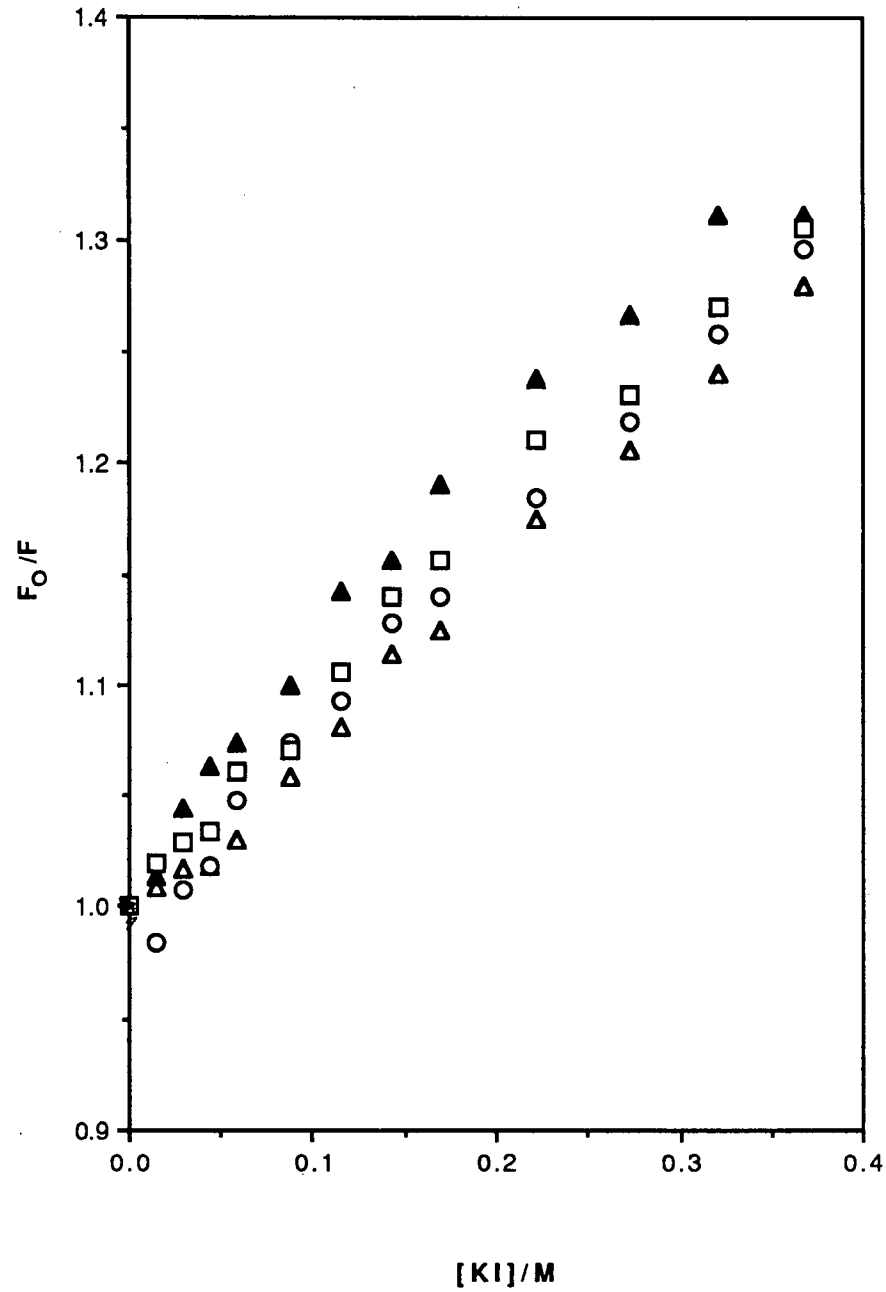

Figure 23: Stern-Volmer plots for iodide quenching of 11:1 (□), 2:1 (○), and 1:1 (▲) actin:ACRG complexes with ACRG (△) Solution conditions were ACRG (1μM), 150mM KCl, 25mM Tris-HCl, 1mM DTT and 1mM $CaCl_2$, pH 8.0. Excitation wavelength was 390nm and emission wavelength was 497nm.

3.2.3 Actin Titration Polarisation Studies

The environment of the acrylodan probe was monitered by polarisation measurements during titration with actin (figure 24). The experiment involved addition of actin (7μM final concentration) to ACRG (1μM initial concentration) and addition of equal volumes of actin buffer (buffer A) to a control sample. The initial solution conditions were 150mM KCl, 25mM Tris-HCl, 1mM DTT and 1mM Ca^{2+}, pH 8.0, at 25°C.

The polarisation value increases on the addition of actin. Such a change confirms complex formation and is likely to be the result of an increase in the size, and so, rotational correlation time for the protein complex to which acrylodan is attached. Polarisation continues to increase with added actin because the excess actin will polymerize onto the nucleus provided by the GA_2 complex formed.

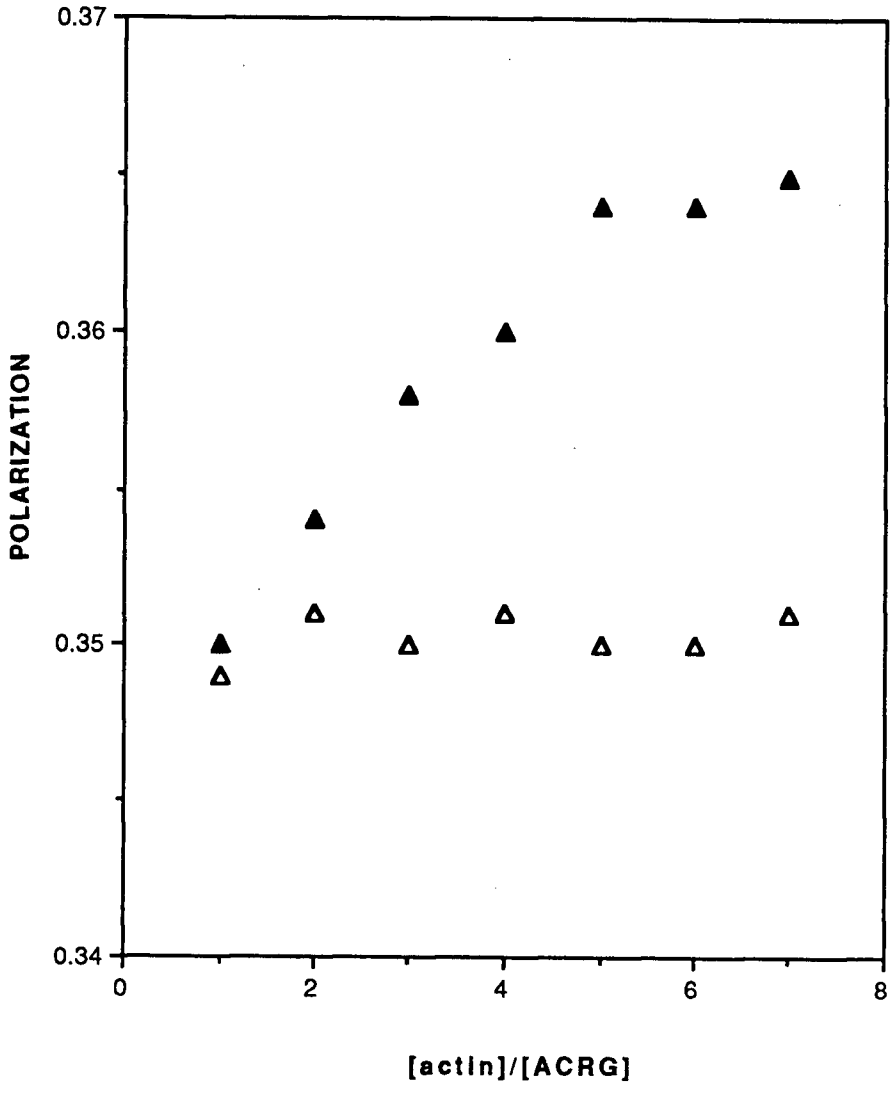

Figure 24: Fluorescence polarisation of ACRG following the addition of monomeric actin. The plot required a pair of identical samples of ACRG (1μM) in 150mM KCl, 25mM Tris-HCl, 1mM DTT and 1mM $CaCl_2$, pH 8.0, at 25°C. To one sample aliquots of actin were added (▲) and to the other equal volumes of actin buffer were added (△). Each polarisation value was the average of 3 measurements and typical standard deviations were ± 0.003. Excitation was at 390nm and emission was at 497nm in both cases.

PART 3: CONCLUSIONS

3.3.1. Summary of Results

Labelling of plasma gelsolin with acrylodan was successful, with an average of about 2 cysteines labelled per gelsolin. The degree of labelling was not significantly influenced by the presence or absence of Ca^{2+}. Viscosity and CD data showed that incorporation of the label did not affect gelsolin's ability to bind actin or the folding of the gelsolin polypeptide chain in a significant manner.

An investigation of the effect of Ca^{2+} on horse plasma gelsolin was undertaken. No effect was seen by CD, however subtle changes could be detected by fluorescence. The presence of Ca^{2+} decreases the fluorescence of ACRG and causes a slight red shift in emission, an increase in sensitivity to quenching and a decreased fluorescence polarisation. These three results are consistent with an increase in exposure of the acrylodan label to solvent in the presence of Ca^{2+} and demonstrate the 'opening' of the gelsolin structure on binding Ca^{2+} that is predicted by the model of Way et al. (1989).

Actin-binding to ACRG was revealed by fluorescence polarisation studies. This interaction was shown to be insensitive to Ca^{2+} by fluorescent intensity titration studies. The decrease in the fluorescence intensity on the binding of actin shown in these titrations is consistant with an observed increase in iodide quenching of actin-ACRG

complexes relative to ACRG alone. This suggests that, as in the case of having free Ca^{2+} present with ACRG, interaction with actin results in increased exposure of the bound acrylodan to the solvent. Such a conclusion would require the acrylodan-labelled site on gelsolin to be distinct from an actin interaction site.

3.3.2. Suggestions for Further Study

Most of the literature on gelsolin, purified from a variety of sources, reports the Ca^{2+} sensitivity of actin binding. An exception to this has been reported for pig plasma gelsolin (Harris and Weeds, 1983). Studies undertaken in this thesis show actin binding by horse plasma gelsolin to be insensitive to Ca^{2+} also. The suggestion by Pope et al. (1989) that Ca^{2+} insensitivity in gelsolin may be the result of the presence of Ca^{2+} in the purification procedure leads to the question of whether or not actin binding with horse plasma gelsolin would be Ca^{2+} sensitive if purified using a method that did not involve Ca^{2+}. Such a method might be developed to take advantage of selective binding and elution of gelsolin using Affi-Gel Blue, as in the final stage of our preparations.

In addition, specific elution of gelsolin from an Affi-Gel Blue column with 1mM ATP suggests a possible, as yet unstudied, role for ATP in the functions of gelsolin. Further investigation of this point is required.

References

1. Bryan, J. (1988) J. Cell Biol., 106, 1553-1562

2. Bryan, J. and Kurth, M.C. (1984) J. Biol. Chem., 259, 11868-11875

3. Cantor, R.C. and Schimmel, P.R. (1980) "Biophysical Chemistry Part II - Techniques for the Study of Biological Structure and Function", W.H. Freeman & Co., San Fransisco.

4. Clark, I.D. and Burtnick, L.D. (1988) Arch. Biochem. Biophys., 260, 595-600

5. Côté, G.P. (1983) Mol. Cell Biol. 57, 127

6. De Rosier, D.J. (1990) Nature, 347, 21-22

7. Doi, Y., Kim, F. and Kido, S. (1990) Biochem., 29,1392-1397

8. Greenfield, N. and Fasman, G.D. (1969) Biochemistry, 8, 4108-4116

9. Harris, E.H. and Weeds, A.G. (1983) Biochemistry, 22, 2728-2741

10. Harris, E.H. and Weeds, A.G. (1984) FEBS, 177, 184-188

11. Ito, H., Yamamoto, H., Kimura, Y., Kambe, H., Okochi, T. and Kishimoto, S. (1990) J. Chromatog., 526, 397-406

12. Janmey, P.A., Iida, K., Yin, H. and Stossel, T.P. (1987) J. Biol. Chem., 262, 12228-12236

13. Janmey, P.A. and Stossel, T.P. (1987) Nature, Vol 325, 362-364

14. Kasai, M., Kawashima, H. and Oosawa, F. (1960) J. Polym. Sci., 44, 51-69

15. Kasha, M.J. (1952) Chem. Phys., 20, 71

16. Korn, E.D. (1978) Proc. Natl. Acad. Sci. USA, 75, 588-599

17. Kwiatkowski, D.J., Stossel, T.P., Orkin, S.H., Mole, J.E., Coltens, H.R. and Yin, H.L. (1986) Nature, 323, 455-458

18. Laemmli, U.K. (1970) Nature, 227, 680-685

19. Lakowicz, J. (1983) "Principles of Fluorescence Spectroscopy", Plenum Press, New York.

20. Lind, S.E., Smith, D.B., Janmey, P.A. and Stossel, T.P. (1988) J. Clinical Invest., 52, 429-434

21. Lind, S.E., Smith, D.B., Janmey, P.A. and Stossel, T.P. (1986) J. Clinical Invest., 78, 736-742

22. Noberg, R., Thorstensson, R., Utter, G. and Fagreus, A. (1979) Eur. J. Biochem., 250, 7485-7891

23. Pollard, T.D. and Craig, S.W. (1982) TIBS (March), 88-92

24. Robinson, R.C. (1990) MSc Thesis, University of British Columbia

25. Pope, J.C., Hinssen, H. and Weeds, A.G. (1989) FEBS Letters, Vol. 259, 1, 185-188

26. Porte, F. and Harricane, M-C. (1986) Eur. J. Biochem., 154, 87-98

27. Prendergast, F.G., Meyer, M., Carlson, G.L., Iida, S. and Potter, J.D., (1983) J. Biol. Chem., 258, 7541-7544

28. Ruiz Silva, B.E. and Burtnick, L.D. (1990) Biochem. Cell Biol., 68, 796-800

29. Saxena, V.P. and Wetlaufer, D.B. (1971) Proc. Natl. Acad. Sci., 68, 969-972

30. Scarborough, V.D., Bradford, H.R. and Ganguly, P. (1981) Biochem. Biophys. Res. Commun., 100, 1314-1319

31. Scopes, R.K. (1987) "Protein Purification - Principles and Practice", Springer-Verlag New York Inc.

32. Spudich, J.A. and Watt, S. (1971) J. Biol. Chem., 246, 4866

33. Stossel, T.P., Chaponnier, C., Ezzell, R., Hartwig, J.H., Janmey, P.A., Kwiatkowski, D.J., Lind, S.E., Smith, D.B., Southwick, F.S., Yin, H.L. and Zaner, K.S. (1985) Annu. Rev. Cell Biol., 1, 353-402, Palo Alto, CA.

34. Straub, F.B. (1942) Studies University of Szeged, 3-15.

35. Stryer, L. (1981) "Biochemistry" Second Edition, W.H. Freeman and Company, San Fransisco.

36. Tellam, R., and Frieden, C. (1982) Biochemistry 21, 3207-3214

37. Tuzimura, K., Konno, T., Meguro, H., Hataiw, M., Marakami, T., Kashiwabara, K., Saito, K., Kondo, Y. and Suzuki, T.M. (1977) Anal. Biochem., 81, 167-174

38. Weeds, A.G., Harris, E.H., Gratzer, W. and Gooch, J. (1986) Eur. J. Biochem., 161, 77-84

39. Way, M., Gooch, J., Pope, B., Weeds, A.G. (1989) J. Cell Biol., 109, 593-605

40. Way, M. and Weeds, A.G. (1988) J. Mol. Biol., 203, 1127-1133

41. Yin, H.L., Kwiatkowski, D.J., Mole, J.E. and Cole, F.S. (1984) J. Biol. Chem., 259, 5271-5276

42. Yin, H.L. and Stossel, T.P. (1979) Nature, 281, 583-586